Pre-Zanclean end of the Messinian Salinity Crisis: new evidence from central Mediterranean reference sections

JOURNAL OF THE GEOLOGICAL SOCIETY
VOL. 178
ISSN 0016-7649
DOI: 10.1144/jgs2020-183

Pre-Zanclean end of the Messinian Salinity Crisis: New evidence from Central Mediterranean reference sections

Speranta-Maria Popescu[1*], William Cavazza[2], Jean-Pierre Suc[3], Mihaela Carmen Melinte-Dobrinescu[4], Nadia Barhoun[5], Christian Gorini[3]

[1]*GeoBioStratData.Consulting, 385 Route du Mas Rillier, 69140 Rillieux la Pape, France*
[2]*Dept. Biological, Geological and Environmental Sciences, University of Bologna, Piazza di Porta San Donato 1, 40126 Bologna, Italy*
[3]*Sorbonne Université, CNRS-INSU, Institut des Sciences de la Terre Paris, ISTeP UMR 7193, 75005 Paris, France*
[4]*National Institute of Marine Geology and Geo-Ecology, 23-25 Dimitrie Onciul Street, 70318 Bucharest, Romania*
[5]*University Hassan II of Casablanca, Faculty of Sciences Ben M'Sik, BP7955 Sidi Othmane, Casablanca, Morocco*
ORCiDs: S.-M.P (0000-0001-5345-395X), W.C. (0000-0002-6030-9689), J.-P.S. (0000-0002-5207-8622), M.C.M.-D. (0000-0003-4716-6844), N.B. (0000-0002-0112-4318), C.G. (0000-0003-3123-4822).
[*]Correspondence (speranta.popescu@gmail.com)

Abstract
The concept of a geologically istantaneous earliest Zanclean reflooding of the Mediterranean Basin after the Messinian drawdown has dominated geological thinking and is ingrained in the scientific literature. The base of the Trubi Formation in southern Italy -formally defined as the Zanclean Global Boundary Stratotype Section and Point (GSSP) at 5.33 Ma- has traditionally been considered as marking the marine reflooding of the Mediterranean. However, several studies provide evidence that marine reflooding occurred prior to the Zanclean GSSP, the most reliable of which comes from southern Calabria. Here, we show that the sedimentary coastal prism cropping out extensively right below the base of the Trubi Formation in this region and correlatable with the Arenazzolo Unit in Sicily, contains a fully marine micropaleontological association of calcareous nannofossils and dinoflagellate cysts, thus pointing to both a high sea level and marine conditions before deposition of the Trubi Formation, i.e., in the latest Messinian.

Introduction

The Mediterranean Messinian Salinity Crisis (MSC) (Selli 1954; Hsü *et al*. 1973*a*) was an extraordinary event as it has been estimated that 5% of the dissolved salt of the global ocean precipitated in a few hundred of thousand years to form a deposit with a volume of more than 1 million km^3 (Ryan 2009) with considerable effects on global atmospheric, oceanographic, and climatic patterns (e.g., Adams *et al*. 1977; Thunnel *et al*. 1987; Sternai *et al*. 2017). After sporadic pioneering work both on land (e.g. Ogniben 1957; Selli 1960; Decima 1964; Ruggieri 1967) and offshore (e.g. Glangeaud *et al*. 1966; Montadert *et al*. 1970), the MSC attracted considerable attention when Deep Sea Drilling Project (DSDP) Leg 13 drilled the top of the evaporites in several western Mediterranean sites and confirmed the existence of an extensive volume of Messinian evaporites (Hsü 1972; Hsü *et al.* 1973a, b). Since DSDP Leg 13, the MSC has been the focus of extensive research resulting in an intense international debate mainly focused on its process, timing, and consequences.

The MSC is now envisioned as a two-step process (Clauzon *et al*. 1996), a scenario largely accepted by the scientific community (CIESM 2008; Roveri *et al*. 2014):

- the first step affected the Mediterranrean peripheral basins (including Sicily) and is characterized by thick deposits of evaporites due to a drop of about 150 m in the Mediterranean Sea level;
- the second step affected the Mediterranean central basins where thick evaporites were deposited as a result of the sea-level drawdown of about 1,500 m, which also caused intense subaerial erosion of the margins, mainly by the rivers.

The specialized community unanimously agrees on a chronology ranging from 5.97 to 5.60 Ma for the 1st step of the MSC (Gautier *et al*. 1994; Krijgsman *et al*. 1999, 2001; Manzi *et al*. 2013). There is a wide agreement about the age of the onset of the paroxysmic 2nd step of the MSC at 5.60 Ma. The end of the MSC, which corresponds to the sudden reflooding of the Mediterranean Basin by Atlantic waters, is usually dated at 5.33 Ma, i.e., the age of the base of the Trubi Formation (Zanclean GSSP) established both in Sicily and southern Calabria (Channell *et al*. 1988; Hilgen and Langereis 1993; Van Couvering *et al*. 2000). Brolsma's proposal (1975, 1976) that marine reflooding occurred prior to the Zanclean (i.e., at the base of the Arenazzolo deposits underlying the Trubi Formation) introduced the first doubts concerning the robustness of the reflooding age at 5.33 Ma. Later, several works provided evidence that marine conditions existed on the Mediterranean margins prior to the beginning of the Zanclean (Cavazza and DeCelles 1998; Londeix *et al*. 2007; Carnevale *et al*. 2008; Bache *et al*. 2012; Pellen *et al*. 2017), a context that was considered likely by Riding *et al*. (1998), Aguirre and Sánchez-Almazo (2004), Cornée *et al*. (2006), Soria *et al*. (2008), Melinte-Dobrinescu *et al*. (2009), Do Couto *et al*. (2014) and Clauzon *et al*. (2015) despite the absence of conclusive relationships with the formal basal Zanclean. According to Bache *et al*. (2012, 2015), the continuous input of Atlantic waters in the almost desiccated Mediterranean central basins started during the late Messinian (at ca. 5.55 Ma) and ended with the sudden and dramatic reflooding estimated at 5.46 Ma. The presence of marine microplankton in the drilled uppermost part of the central evaporites (2nd step of the MSC) has long been known (Cita 1973; Cita *et al*. 1978; Iaccarino and Bossio 1999) although its reliability is still under discussion (Popescu *et al*. 2015). Marine reflooding of the Mediterranean Basin is interpreted as occurring at either 5.46 Ma (Bache *et al*. 2015; Clauzon *et al*. 2015; Popescu *et al*. 2015; Suc *et al*. 2015) or 5.33 Ma (Roveri *et al*. 2014; Krijgsman *et al*. 2018). Although not directly linked with the purpose of this paper, but closely associated with the reference sections in Sicily, the ongoing debate concerning Lago Mare (LM) needs clarifying: characterized by the occurrence of Paratethyan species in the Mediterranean, one episode is considered as closing the MSC (Roveri *et al*. 2014) and three distinct episodes have been chronologically distinguished by Clauzon *et al*. (2005) and Popescu *et al*. (2015).

Southern Calabria provides the most robust evidence of a pre-Zanclean coastal sedimentary prism (DeCelles and Cavazza 1992, 1995; Cavazza and DeCelles 1998), exposed immediately below the Trubi Formation in the areas of Monte Singa (Zijderveld *et al*. 1986; Hilgen 1987, 1991; Hilgen and Langereis 1993) and Capo Spartivento (Channell *et al*. 1988), which are among the reference sections for the establishment at Eraclea Minoa of the Miocene–Pliocene boundary (Van Couvering *et al*. 2000). Our target was to find marine microfossils (possibly biostratigraphic markers) within the Calabrian coastal prism underlying the formal Lower Pliocene, with the aim of proving that the Mediterranean reflooding occurred significantly before the earliest Zanclean.

Geological framework

The Calabria-Peloritani Terrane (CPT) is an exotic terrane composed of several nappes piled up during Alpine-age deformation and involving an ancient crystalline basement affected by the Hercynian orogeny (Amodio-Morelli *et al*. 1976; Bonardi *et al*. 2001). Although originally part of the European southern continental margin, the CPT rifted off the margin in the Oligocene after the Alpine collision and drifted southeastward during the Neogene until it collided with the African continental margin in the Langhian (early Middle Miocene) time (Alvarez *et al*. 1974; Dercourt *et al*. 1985; Malinverno and Ryan 1986; Dewey *et al*. 1989; Gueguen *et al*. 1998; Jolivet and Faccenna 2000; Cavazza *et al*. 2004). The Ionian coast of southeastern Calabria is arguably the only place in western and central Mediterranean regions where an Alpine-age continental collision has not occurred. In this region, northwestward subduction of the Ionian Neotethyan oceanic lithosphere is still underway, albeit passively, under the Calabrian microplate, as indicated by a northwestward dipping subduction plane (e.g. Spakman and Wortel 2004) and by the mostly Quaternary calcalkaline volcanism of the Aeolian Islands (e.g. De Astis *et al*. 2003).

The Ionian forearc basin is located between the subduction zone and the CPT basement units cropping out on land (Fig. 1B-C). The term ‘‘forearc’’ is used here to define the location of the basin between the Ionian subduction zone and the corresponding calcalkaline volcanic arc of the Aeolian Islands, with no implications as to the mechanism responsible for the development of the basin. The proximal portion of the Ionian forearc basin fill crops out extensively along the southeastern coast of Calabria due to rapid uplift of the CPT since the Middle Pleistocene (Tortorici *et al*. 1995). This uplift has been interpreted as resulting from unflexing of the Ionian foreland lithosphere upon break-off of its subducted slab following the docking of the CPT (e.g. Spakman and Wortel 2004).

Along the Ionian coast of southeastern Calabria, the proximal portion of the forearc basin fill is >2,000 m thick and comprises upper Oligocene to Quaternary lithostratigraphic units (Figs. 2, 3) (Cavazza *et al*. 1997; Bonardi *et al*. 2001), with an overall upward-shallowing trend. The basal part of the basin fill is formed by uppermost Chattian–Burdigalian turbidite deposits of the Stilo–Capo d’Orlando Formation (Bonardi *et al*. 1980; Cavazza 1989; Cavazza and DeCelles 1993) conformably overlain by a large-scale olistostrome mélange informally named *Varicoloured clays* (Cavazza and Barone 2010). The latter is overlain by the San Pier Niceto Formation, a Serravallian-Tortonian succession of proximal marine conglomerate, sandstone and mudstone (Critelli *et al*. 2015a, b). The Messinian stratigraphy is described in more detail below. The carbonate-marl rhythms of the Zanclean Trubi Formation onlap all the older lithostratigraphic units and are, in turn, overlain by Upper Pliocene-Lower Pleistocene shallow marine calcarenite, siliciclastic sandstone, and mudstone. Beach and fluvial terraces discontinuously cover older formations and can be found at elevations more than 1,000 meters above sea level, indicating a dramatic uplift of the Calabrian block during the last 700 ka (e.g. Tortorici *et al*. 1995).

Messinian physical stratigraphy and sedimentological facies

This section mostly refers to previously published data (DeCelles and Cavazza 1992; Cavazza and DeCelles 1998) that are briefly summarized here. The Messinian evaporitic and post-evaporitic succession that crops out along the Ionian coast of southeastern Calabria comprises three units

(Figs. 2 and 3). Lower Messinian evaporites and pelites (Unit 1) are conformable or slightly unconformable with respect to the underlying units, whereas the upper Messinian siliciclastic deposits (units 2 and 3) are mainly sub-horizontal, essentially undeformed, and are separated from the underlying succession by an angular unconformity or a laterally equivalent disconformity. Some of the more complete outcrops of the Messinian post-evaporitic succession are located between the towns of Guardavalle to the north and Caulonia to the south (Fig. 1). In the present study, we mainly focused on such outcrops but also conducted observations on the Messinian stratigraphy over ca. 80 km along depositional strike.

The limestone-gypsum succession of Unit 1

Unit 1 (*Formazione di Cattolica* of Critelli *et al.* 2015*a*, *b*) is made of a thin discontinuous limestone-gypsum succession conformably overlying the Serravallian–Tortonian succession of the San Pier Niceto Formation and the lowermost, pre-evaporitic Messinian (Figs. 3, 4). The maximum total thickness of Unit 1 is ca. 100 m. In the study area, the limestone member (known elsewhere as *Calcare di Base*; Ogniben 1957) is largely recrystallized, and its original fabric is difficult to recognize. It is composed of micritic-microsparitic aggregates, probably pseudo-oolites related to algal activity (see Decima *et al*. 1988), or fecal pellets, set in microsparitic cement. In other areas, this lithostratigraphic unit comprises abundant filament-like peloids, arguably due to the activity of cyanobacteria (Guido *et al*. 2007) similar to those described in the Messinian evaporites by Vai and Ricci Lucchi (1977) and Manzi *et al*. (2011). Thin layers of macro- and mesocrystalline gypsum with swallow-tail twinning are occasionally present within the limestone. The gypsum member of Unit 1 discontinuously overlies the limestone member described above. It is made of epiclastic gypsum-arenite and gypsum-rudite; no primary gypsum was found.

The fanglomerates of Unit 2

Unit 2 (*Formazione di Monte Canolo* of Critelli *et al*. 2015*a*, *b*) is up to 80 m thick and thins progressively southeastward (Fig. 5) or southward (Fig. 6) up to <10 m, although the actual pinch-out is not visible. It consists of poorly to medium sorted cobble to boulder conglomerate. Average maximum clast size in individual beds ranges from 15 to 160 cm; no clear vertical trends in grain-size are visible although the bulk of Unit 2 fines systematically eastward. The most common conglomerate lithofacies are generally clast supported and comprise horizontally stratified, imbricated and structureless conglomerate. At a larger scale, the bedding is crudely lenticular. Imbrications indicate south-southeastward paleoflow. Unit 2 is interpreted as deposits of stream-dominated alluvial fans (Cavazza and DeCelles 1998). Conglomerate clast composition is dominated by plutonic and subordinate phyllitic rocks, with small amounts (<5%) of Mesozoic and Lower Cenozoic carbonates. Taken together, compositional and paleocurrent data indicate that the upper Messinian fanglomerates of Unit 2 were derived from the Hercynian basement complex directly to the west-northwest of the study area.

The sedimentary prism of Unit 3

The thickness of Unit 3 in the outcrops ranges from 0 to 52 m. In the Guardavalle fence diagram (Fig. 5), Unit 3 pinches out south-eastward, whereas in the Caulonia fence diagram, it can be seen pinching out north-westward and its eastward continuation lies in the subsurface (Fig. 6). Based on stratigraphic/sedimentological measurements and field observations, this unit has a ribbon geometry elongated along the strike of the latest Messinian depositional system and nearly parallel to the present-day coastline. Based on geometric considerations, the width of Unit 3 perpendicular to depositional strike is estimated to be 3–4 km. A variety of sedimentological facies and facies associations are observed in Unit 3 (e.g., Figs. 7, 8). The following is a concise description; interested readers should refer to DeCelles and Cavazza (1992) and Cavazza and DeCelles (1998) for details.

The stratigraphy of Unit 3 is characterized by poorly cemented, very fine- to coarse-grained sandstone arranged in vertically coherent sequences typically consisting of structureless medium- to coarse-grained sandstone, overlain by medium- to coarse-grained trough cross-stratified and hummocky cross-stratified (HCS) sandstone, in turn overlain by low-angle, laminated, very well sorted sandstone (e.g. Fig. 7). An irregular erosional surface, overlain by coarse-grained trough cross-stratified sandstone or imbricated pebble conglomerate, forms the upper part of a few of these sequences. These recurring sequences have been interpreted as progradational shallow marine to fluvial parasequences (DeCelles and Cavazza, 1992; Cavazza and DeCelles, 1998). The shallow marine parts of these sequences consist of a storm-dominated surf zone, beach, and beach-ridge deposits. Where present, the beach-ridge deposits comprise large-scale, low-angle, bidirectional cross-stratification, and are associated with interlayered claystone and siltstone (or very fine-grained sandstone) with flaser bedding, starved ripples and wavy lamination. This association of finer grained lithofacies has been interpreted as the deposits of shallow lagoons on the landward sides of beach ridges (DeCelles and Cavazza, 1992; Cavazza and DeCelles, 1998).
Overall, the Messinian sediments of Unit 3 in eastern Calabria were deposited along an east-facing shoreline rather resembling the modern shoreline, where ephemeral gravelly braided streams drain the nearby highlands and form small braid-delta systems along an otherwise straight and open shoreface dominated by storm-wave-driven currents and negligible tidal processes. Spits parallel to the shore occasionally separate the alongshore deflected fluvial channels from the open shoreface and shallow lagoons develop where fluvial channels are abandoned. Locally, a thin dark clayey bed caps Unit 3 deposits (sections A2, A4, C4; Figs. 6, 8, 10), in sharp colour contrast to the immediately overlying white first carbonate bed of the Trubi Formation. The interpretation of this distinctive bed, shown in the sections of Figure 6, is proposed below.

Overall interpretation of Messinian stratigraphy
Despite local erosional features, the evaporites of Messinian Unit 1 are substantially concordant with the underlying succession and document continuous evolution from open marine (Tortonian) to progressively restricted (early Messinian) environments. Conversely, a sharp angular unconformity separates the coarse-grained conglomerates of Messinian Unit 2 from all underlying units, including the Hercynian basement complex and the pre-conglomerate Cenozoic sedimentary succession (Figs. 3, 4). The older Cenozoic rocks generally dip 30–50º eastward, and must have been rotated after Tortonian time, but prior to deposition of the Messinian fanglomerates. This geometric relationship demonstrates that deposition of the Messinian fanglomerates (Unit 2) cannot merely be the product of the lowering of the base level due to the desiccation of the Mediterranean Sea, as also demonstrated by the fact that such conglomerates are not restricted to incised valleys but are also preserved in a structurally and topographically high position in the Calabrian orogenic wedge. In addition, this unconformity is widespread in the Mediterranean region (e.g. Decima and Wezel 1973; Fabbri and Curzi 1979; Dondi 1985; Kastens *et al*. 1990; Butler *et al*. 1995; Riding *et al*. 1998; Braga *et al*. 2003), clearly pointing to intra-Messinian tectonic activity that significantly modified the regional physiography (Jolivet *et al*. 2006).

Micropaleontology: methods and results
Seventeen samples were collected for micropaleontological analyses near Guardavalle focusing on easily accessible clayey and silty facies within the upper part of Unit 3 and the lowermost layers of the Trubi Formation (Figs. 5–6). Information on the locations sampled is provided in Table 1: most of the samples came from Unit 3 (location G3: samples 1–3; location G5: samples 1–2; location A2: sample 1; location A4: sample 1; location C4: samples 1–6; Careri : sample 1); a few samples came from the lowermost Trubi Formation (location A2: samples 2–3; Careri: sample 2). Careri (Fig. 8) is located outside the mapped area in Figure 1.
The methods used for microfossil extraction and identification were as follows:

- calcareous nannofossils: 2 grams of sediment were used to prepare smear slides; the calcareous nannofossil analyses were performed using a light polarizing microscope at 1600× magnification; their taxonomic identification follows Perch-Nielsen (1985) and Young (1998);
- foraminifera: 10–15 grams of sediment were disaggregated in a warm solution of sodium carbonate (Na_2CO_3); the residue was sieved at 50 μm, 150 μm and 250 μm, and all the material was analyzed and identified following Iaccarino and Premoli Silva (2007);
- dinoflagellate cysts: acid treatments using HCl, HF, and again HCl on 10 to15 grams of sediment followed by concentration in $ZnCl_2$ (density 2.0) and sieving at 10 μm; a 50 μl volume of residue was mounted in glycerol and examined under a light microscope (magnification: 1000×). Identification was based on the database of Williams *et al*. (2017).

Tables 2–4 list the results for calcareous nannofossils, planktonic foraminifera and dinoflagellate cysts, respectively.

Calcareous nannofossils

The samples from Unit 3 yielded a diversified calcareous nannofossil assemblage, evidence for an open marine environment (samples G3-1–3, G5-1–2, A2-1, A4-1, C4-1–6, Careri-1; Figs. 5–6). Table 2 lists the occurrence of some species of biostratigraphic significance: *Discoaster quinqueramus*, *Orthorhabdus* (ex *Triquetrorhabdulus*) *rugosus*, and *Ceratolithus acutus* (Fig. 9). The highest occurrence (HO) of *D. quinqueramus* is suggested at about 5.53 Ma (Zeeden *et al*. 2013), but its extinction age in the Mediterranean has not been defined precisely. The lowest occurrence (LO) of *C. acutus* is indicated between 5.35 Ma (Raffi *et al*. 2006; Anthonissen and Ogg 2012) and 5.368 Ma (Zeeden *et al*. 2013). The two species were not recorded in the same samples, suggesting an age between 5.53 and 5.35 Ma for Unit 3. This is in agreement with the occurrence of *O. rugosus* (HO at 5.28 Ma: Raffi *et al*. 2006; Anthonissen and Ogg 2012). It should be noted that *Nicklithus amplificus* was recorded in a few samples from Unit 3 (Table 2) but must be considered as reworked because its HO is dated at about 5.94 Ma (Raffi *et al*. 2006; Anthonissen and Ogg 2012). The samples from the Trubi Formation (samples A2-2–3, Careri-2; Figs. 5–6) yielded a somewhat less diversified calcareous nannofossil assemblage, showing the occurrence of *O. rugosus* at location A2 (Table 2), consistent with the astronomical age of 5.30 Ma ascribed to the top of the first carbonate-marl precession cycle in the nearby Singa section in agreement with the base of the *Sphaeroidinellopsis* Acme (Van Couvering *et al*. 2000; Lirer *et al*. 2019). Figure 10 summarizes the calcareous nannofossil biostratigraphy and the inferred chronostratigraphy of Unit 3.

Planktonic foraminifera

Only three samples from the Trubi Formation from the location A2 and Careri (Fig. 6) yielded planktonic foraminifera that are on the whole, abundant (Table 3). This planktonic microfauna is evidence of normal marine conditions. Combined with the occurrence of *Sphaeroidinellopsis seminulina* and the absence of typical individuals of *Globorotalia margaritae*, its composition is consistent with the location of the samples in the lowermost Zanclean, i.e., before the base of the *Sphaeroidinellopsis* Acme Zone (5.30 Ma; Lirer *et al*. 2019).

Dinoflagellate cysts

Six samples from Unit 3 (samples A4-1, C4-1–2, C4-4–6; Fig. 6) yielded a dinoflagellate cyst flora (Table 4). The assemblage in sample A4-1 is dominated by *Lingulodinium machaerophorum* and *Homotryblium* sp., thus indicating coastal to lagoonal conditions. The assemblage from location C4 shows an interesting progression, from very poor (samples 1–2) to very rich (sample 6) in terms of diversity and the number of specimens. The latter, characterized by abundant cysts of

Impagidinium patulum and *I. sphaericum* (Fig. 9), is evidence for full open marine conditions while the underlying sample C4-4 rather points to a coastal environment. No dinoflagellate cyst originating from the Paratethys, constituting the Lago Mare biofacies as described by Popescu *et al*. (2015), was recorded in the samples studied here.
Overall, the clayey thin microfossiliferous beds of Unit 3 (Figs. 5–6) may illustrate several successive minor sea-level rises, especially the uppermost one and its darker termination that immediately precedes the Trubi Formation.

Discussion
Previous studies have shown that the Messinian succession in southeastern Calabria was deposited in response to complex interactions between eustacy and tectonics (DeCelles and Cavazza 1995; Cavazza and DeCelles 1998). The abrupt vertical compositional change and angular unconformity between the evaporites of Unit 1 and the coarse-grained siliciclastic fanglomerates of Unit 2 were produced by intra-Messinian thrusting in the upper part of the Calabrian orogenic prism. Reworking of these clastics during the marine reflooding of the Mediterranean Basin produced the uppermost Messinian deposits of Unit 3, a costal prism that was deposited by episodically prograding sandy shoreface systems (DeCelles and Cavazza 1992; Cavazza and DeCelles 1998). The subsequent general onlap of the pelagic oozes of the Trubi Formation at the Miocene–Pliocene boundary resulted from an additional sea-level rise, that drowned all pre-existing sedimentary deposits, somewhat reducing the land area and the terrigenous input to the basin, thereby promoting carbonate sedimentation in the basin (Butler *et al*. 1995; Bache *et al*. 2012).
Considering the large vertical distribution of samples containing marine microplankton (Figs. 5–6), the micropaleontological dataset presented in this paper confirms that Unit 3 was deposited in open marine conditions, as previously suggested by Cavazza and DeCelles (1998) based on purely stratigraphic and sedimentologic grounds. Our results concerning the Calabrian Unit 3, the novelty of which is the evidence of marine microplankton including robust biostratigraphic markers (such as *Ceratolithus acutus* and *Orthorhabdus rugosus*), support the hypothesis that the marine reflooding that put an end to the MSC in the Mediterranean occurred significantly before the beginning of the Zanclean Stage corresponding formally to the base of the Trubi Formation.
The stratigraphy described by Karakitsios *et al*. (2017) in their Kalamaki East section on Zakynthos Island is particularly relevant to this discussion. In that area, a thin dark shale bed overlies a laminated greenish marly interval referred to as the Lago Mare biofacies above the Messinian Erosional Surface. Several samples from these two layers contain *Ceratolithus acutus* among other species of calcareous nannofossils and planktonic foraminifera. The dark shale bed is immediately overlain by the first carbonate layer of the Trubi Formation well dated by both micropaleontological and magnetostratigraphic means (Karakitsios *et al*. 2017: sample KAL 134 – fig. 16, table S1–S2). This context closely resembles the succession described by Bache *et al*. (2012) and Popescu *et al*. (2015) at the Zanclean GSSP (Eraclea Minoa, S Sicily) comprising, from bottom to top: (i) the Messinian Discontinuity (the surface is considered to be due to marine reflooding), (ii) the onlapping Arenazzolo silty Unit (both including Paratethyan and marine dinoflagellate cysts) topped by a thin dark clayey bed, and finally (iii) the Trubi Formation. Accordingly, a comparison of the latest Messinian–earliest Zanclean succession of the classic locations in southern Calabria and southern Sicily is needed because they probably both belong to a similar paleogeographic context along the front of the Calabrian accretionary wedge corresponding to relatively coastal conditions (Fig. 12).

Calabria vs. Sicily latest Messinian–earliest Zanclean succession
The comparison focuses mainly on Calabrian Unit 3 (Cavazza and DeCelles 1998) and the Sicilian Arenazzolo Unit (Ogniben 1957; Bache *et al*. 2012; Popescu *et al*. 2015), i.e., the units located stratigraphically between the Messinian evaporites at the bottom and the Trubi Formation at the top. In Calabria, the contact between Unit 3 and Unit 2 (fanglomerate) is sharp (Fig. 7) and can be

interpreted as a ravinement surface delimiting the base of the sedimentary prism of Unit 3 (Figs. 5–6; Cavazza and DeCelles 1998). In several places (Fig. 6), a clayey dark bed of variable thickness ends Unit 3, the uppermost 3–5 centimeters of which are darker and are in sharp colour contrast with the whitish first carbonate bed of the Trubi Formation (Figs. 10, 13). As argued above, this dark layer, observed in the Caulonia region (locations A4 and C4) and at Careri (Figs. 6, 8, 10), rich in marine microplankton (Tables 2, 4), results from a sea-level rise and represents maximum flooding. At Eraclea Minoa in Sicily, the Arenazzolo and Trubi formations can be traced for quite a distance. Here, a well-marked discontinuity was evidenced at the base of the Arenazzolo Unit, called the 'Messinian Discontinuity' by Popescu *et al*. (2009, 2015) and Bache *et al*. (2012). In southern Calabria, this discontinuity marks a clear separation between units 2 and 3. Its smooth morphology and wide regional extent lead us to interpret this surface as resulting from transgressive ravinement (i.e. a wave-cut surface; see modern and past examples in Bache *et al*. 2012). At Eraclea Minoa, this surface marks the base of an assemblage of inner-to-outer-shelf dinoflagellate cysts also containing Paratethyan species (Bache *et al*. 2012). The sedimentary gap has been interpreted as corresponding to the second, paroxysmal, step of the MSC (Clauzon *et al*. 1996; Bache *et al*. 2012). In this paper, we therefore call this discontinuity 'transgressive ravinement surface' (TRS) (Fig. 13) as defined by Catuneanu and Zecchin (2013). The overlying Arenazzolo Unit is thus suggested as marking the marine reflooding of the Mediterranean Basin, as also shown by a marine, although relatively poor, calcareous nannofossil assemblage (Bache *et al*. 2012), in line with earlier suggestions (Brolsma 1975, 1976). Bache *et al*. (2012) proposed that marine reflooding occurred at 5.46 Ma~~,~~ based on a tentative cyclostratigraphy. This age is consistent with the LO of *Discoaster quinqueramus* and the FO of *Ceratolithus acutus* (Fig. 10) for the reflooding event recorded in Calabria. This event must be regarded as a sudden marked rise of the Mediterranean Sea level, which was estimated at ca. 500 m by Bache et al. (2012) (Fig. 13). In addition, the Arenazzolo Unit corresponds to the third Lago Mare episode (LM3: high sea-level Paratethys–Mediterranean exchanges; Clauzon *et al*. 2005) closely linked to marine reflooding (see for details: Popescu *et al*. 2015). Like the Calabrian Unit 3, Arenazzolo ends with a 50 cm-thick clayey layer, the uppermost centimeters of which are darker (Fig. 13), that we interpret as a condensed interval representing a maximum flooding event.

Paleoenvironmental and paleogeographic inferences

The proposed chronostratigraphic correlation of the Sicilian Arenazzolo Unit with the Calabrian Unit 3 (Fig. 13) and their comparison leads us to paleoenvironmental interpretations that can be integrated in up-to-date knowledge of paleogeography.

The latest Messinian pre-Trubi siliciclastic units of Sicily and Calabria have a consistent stratigraphic position but vary in thickness and sedimentary facies. For example, Calabrian Unit 3 comprises paleoenvironments ranging from fully marine to continental (DeCelles and Cavazza 1992, 1995; Cavazza and DeCelles 1998) and varies in thickness from 0 to 52 meters (Figs. 5–6). The extensive outcrops of Unit 3 three-dimensionally delineate a ribbon-shaped sedimentary body, elongated along the strike of the Messinian depositional system, virtually parallel to the present-day coastline. This depositional system developed over a rugged paleotopography (hence the lateral variations in facies, thickness, and stacking pattern) and prograded into a deep body of water (hence a wide accommodation space). Conversely, the Arenazzolo appears to be rather uniformly characterized by brackish to marine paleoenvironments (Bache *et al*. 2012) and its thickness is limited and somewhat more uniform over the entire Sicilian Caltanissetta Basin (Decima and Wezel 1973). This suggests a limited accommodation space, i.e., shallower water than in Calabria. The calcareous nannofossil assemblage leads to the same conclusion, being more abundant and diversified in Unit 3 than in the Arenazzolo (Bache *et al*. 2012). Deeper conditions offshore South Calabria are supported by paleogeographic reconstructions showing the proximity of the Ionian Basin where evaporites were deposited during the 2nd step of the MSC (Fig. 12; Jolivet *et al*. 2006; Haq *et al*. 2020; Manzi *et al*. 2020). Evaporites of the Caltanissetta Basin have long been

considered to belong to the deep central Mediterranean basins (i.e., deposited during the 2nd step of the MSC). Clauzon *et al*. (1996) and Bertini *et al*. (1998) placed them in the 1st step of the MSC. Today, there is a wide consensus for ascribing them to a peripheral basin, probably deeper than the more internal peri-Mediterranean basins such as Sorbas (Clauzon *et al*. 1996; CIESM 2008; Roveri *et al*. 2014). An onshore–offshore study in Tunisia supports the two-step MSC scenario (Clauzon *et al*. 1996): peripheral evaporites of the 1st step show a gypsum-anhydrite-halite succession (borehole Carthage 1; Fig. 12) similar in both thickness and structure to that of Sicily (borehole Porto Empedocle 38; Fig. 12), cut by the deep fluvial canyon of the Medjerda River (Fig. 12) demonstrating the 2nd step of the MSC (El Euch-El Koundi *et al*. 2009). This evidence implies that, at that time, the Sicily–Tunisia marine domain should be considered a peripheral basin including some deeper parts (El Euch-El Koundi *et al*. 2009). A similar conclusion was proposed by Micallef *et al*. (2019) for the Sicily–Tunisia domain which, during the 2nd step of the MSC, was separated from the Ionian Basin by the eroded Malta Escarpment. The peripheral status of the Sicilian Basin is also supported by the erosional cutting caused by the Salso River at the northern edge of the basin (Fig. 12; El Euch-El Koundi *et al*. 2009; Maniscalco *et al*. 2019). We conclude that the latest Messinian successions of southern Calabria and Sicily, although deposited in bathymetrically rather different conditions, likewise recorded the pre-Zanclean reflooding of the Mediterranean Basin.

Revisited significance of some geological formations

Three Lago Mare episodes, mainly characterized by the influx of Paratethyan dinoflagellates (i.e., transported by surface waters), have been identified during the latest Messinian–earliest Zanclean time interval (Clauzon *et al*. 2005; Popescu *et al*. 2009, 2015; Do Couto *et al*. 2014). The first and the third episodes (LM1–LM3) -recorded both in peripheral and central basins- occurred respectively, at the end of the first MSC step and during the post-crisis marine reflooding and were caused by high sea-level exchanges between the Mediterranean and Paratethys. The second episode (LM2) -recorded only in the central basins, in both of the western and eastern Mediterranean- occurred right after the peak of the MSC and is interpreted as resulting from an overflow from the perched Aegean realm that pooled Paratethyan waters (Popescu *et al*. 2015). The Eraclea Minoa stratigraphic section records the LM1 and LM3 episodes (Fig. 13; see for details: Popescu *et al*. 2009, 2015; Bache *et al*. 2012), the latter being located within the Arenazzolo. As a consequence, we expected to find Paratethyan dinoflagellate cysts in the Calabrian Unit 3, but our search was unsuccessful. The absence of Paratethyan dinoflagellate cysts in the south Calabria Unit 3 could be explained by the high energy sediment input from the continent resulting in thinner clayey deposits compared to thick coarser clastics (Figs. 5–6).

The integration of preexisting stratigraphic, sedimentologic, and paleontological data from the latest Messinian Unit 3 of southeastern Calabria and the correlative Arenazzolo Unit in Sicily confirm that fully marine conditions were reestablished in the Mediterranean Basin well before the initial deposition of the Trubi Formation, traditionally considered as the first marine unit after the end of the MSC (e.g. Van Couvering *et al*. 2000, and references therein). Earlier reports of the occurrence of pre-Trubi marine microplankton (Brolsma 1975, 1976; Londeix *et al*. 2007) were dismissed, possibly because they challenged the widely accepted scenario of the 'Zanclean deluge', i.e., a virtually synchronous flooding of the Mediterranean Basin that gained acceptance within the scientific community. This 'deluge' is thought to be marked by the base of the Trubi Formation, providing a convenient datum for the formal establishment of the base of the Pliocene. However, in the last few years, a growing body of evidence points to a more complex sequence of events, with at least two stages in the refilling of the Mediterranean Basin (Bache *et al*. 2012). Based on micropaleontological data, the present study validates the hypothesis that the uppermost Messinian marine deposits below the Trubi Formation represent complete reflooding of the Mediterranean Basin followed by further sea-level rise recorded by the Trubi Formation driven by glacioeustacy (Miller *et al*. 2011; Gorini *et al*. 2014).

Conclusion

In southern Calabria, a coastal sedimentary prism (Unit 3) characterizes the latest Messinian and is overlain by the Zanclean Trubi Formation, traditionally considered as the reestablishment of fully marine conditions in the Mediterranean Basin following the Messinian Salinity Crisis. Analyses of physical stratigraphy and sedimentary facies previously evidenced that Unit 3 marks a transgressive event ending with a maximum flooding condensed interval just below the highstand recorded by the Trubi Formation. Calcareous nannofossils and dinoflagellate cysts found in the present study show that this unit is fully marine. We thus conclude that the marine reflooding of the Mediterranean Basin that ended the MSC occurred significantly before the beginning of the Zanclean Stage. The Sicilian Arenazzolo is time equivalent of the Calabrian Unit 3. Sharp lithological breaks do not correspond to the most important environmental changes, such as the passage from a terrigenous succession to carbonate sedimentation probably promoted by continuous sea-level rise. The Trubi Formation is not the expression of the post-MSC marine reflooding but denotes only a glacio-eustatic rise in sea level. The marine reflooding significantly predates the Zanclean GSSP. An age of 5.46 Ma is thus conceivable for the end of the Messinian Salinity Crisis, more than 100 kyrs before the beginning of the Zanclean.

Acknowledgements

Portions of this study developed from past collaboration between W. Cavazza and P.G. DeCelles and from the geological mapping of several students at the University of Bologna (M. Dall'Olmo, S. Gangemi, M. Macchiarola, L. Zanarini, A. Zanutta). N. Loget and J. Van Den Driessche participated in a preliminary reconnaissance. D. Do Couto reviewed an earlier version of this manuscript. W.B.F. Ryan and two other anonymous referees reviewed the manuscript and contributed significantly to its improvement.

Funding

Funding for this research was provided over the years by ISTeP, the GRI South Tethys (University P. & M. Curie – Total), the TerMex Program (MISTRALS), CNR, MIUR, NATO, and the University of Bologna.

Author contributions

S.-M.P.: supervision of micropaleontological studies, dinoflagellate cysts analyses, writing (equal);
W.C.: conceptualization of the research, stratigraphic-sedimentologic study in the field, writing - original draft (equal);
J.-P.S.: sampling in the field, correlations at the Mediterranean scale, writing - original draft (equal);
M.C.M.-D.: calcareous nannofossil analyses, review;
N.B.: planktonic foraminifer analyses, review;
C.G.: funding acquisition, onshore-offshore relationships in the Central Mediterranean, review.

Data availability statement

All data generated or analysed during this study are included in this article.

References

Adams, C.G., Benson, R.H., Kidd, R.B., Ryan, W.B.F. and Wright, R.C. 1977. The Messinian salinity crisis and evidence of late Miocene eustatic changes in the world ocean. *Nature*, **269**, 383–386.

Aguirre, J. and Sánchez-Almazo, I.M. 2004. The Messinian post-evaporitic deposits of the Gafares area (Almería-Níjar basin, SE Spain). A new view of the "Lago-Mare" facies. *Sedimentary Geology*, **168**, 71–95, doi:10.1016/j.sedgeo.2004.03.004

Alvarez, W., Cocozza, T. and Wezel, F.C. 1974. Fragmentation of the Alpine orogenic belt by microplate dispersal. *Nature*, **248**, 309–314.

Amodio Morelli, L., Bonardi, G., Colonna, V., Dietrich, D., Giunta, G., Ippolito, F., Liguori, V., Lorenzoni, S., Paglionico, A., Perrone, V., Piccarreta, G., Russo, M., Scandone, P., Zanettin-Lorenzoni, E. and Zuppetta, A. 1976. L'arco calabro-peloritano nell'orogene appenninico-maghrebide. *Memorie della Società geologica italiana*, **17**, 1–60.

Anthonissen, D.E. and Ogg, J.G. 2012. Cenozoic and Cretaceous biochronology of planktonic foraminifera and calcareous nannofossils. *In*: Gradstein, F.M., Ogg, J.G., Schmitz, M.D. and Ogg G.M. (eds) *The geologic time scale 2012*. Elsevier, 1083–1127.

Bache, F., Gargani, J., Suc, J.-P., Gorini, C., Rabineau, M., Popescu, S.-M., leroux, E., Do Couto, D., Jouannic, G., Rubino, J.-L., Olivet, J.-L., Clauzon, G., Dos Reis, A.T. and Aslanian, D. 2015. Messinian evaporite deposition during sea level rise in the Gulf of Lions (Western Mediterranean). *Marine and Petroleum Geology*, **66**, 262–277, http://dx.doi.org/10.1016/j.marpetgeo.2014.12.013

Bache, F., Popescu, S.-M., Rabineau, M., Gorini, C., Suc, J.-P., Clauzon, G., Olivet, J.-L., Rubino, J.-L., Melinte-Dobrinescu, M.C., Estrada, F., Londeix, L., Armijo, R., Meyer, B., Jolivet, L., Jouannic, G., Leroux, E., Aslanian, D., Dos Reis, A.T., Mocochain, L., Dumurdzanov, N., Zagorchev, I., Lesic, V., Tomic, D., Çağatay, M.N., Brun, J.-P., Sokoutis, D., Csato, I., Ucarkus, G. and Çakir, Z. 2012. A two-step process for the reflooding of the Mediterranean after the Messinian Salinity Crisis. *Basin Research*, **24**, 125–153, doi:10.1111/j.1365-2117.2011.00521.x

Bertini, A., Londeix, L., Maniscalco, R., Di Stefano, A., Suc, J.-P., Clauzon, G., Gautier, F. and Grasso, M. 1998. Paleobiological evidence of depositional conditions in the Salt Member, Gessoso-Solfifera Formation (Messinian, Upper Miocene) of Sicily. *Micropaleontology,* **44**, 413–433.

Bonardi, G., Giunta, G., Perrone, V., Russo, M., Zuppetta, A. and Ciampo, G. 1980. Osservazioni sull'evoluzione dell'arco calabro-peloritano nel Miocene inferiore: la Formazione di Stilo–Capo d'Orlando. *Bolletino della Società geologica italiana*, **99**, 365–393.

Bonardi, G., Cavazza, W., Perrone, V. and Rossi, S. 2001. Calabria-Peloritani terrane and northern Ionian Sea. *In*: Vai, G.B. and Martini, I.P. (eds) *Anatomy of an Orogen: the Apennines and Adjacent Mediterranean Basins*. Kluwer Academic Publishers, 287–306.

Braga, J.C., Martín, J. and Quesada, C. 2003. Patterns and average rates of late Neogene–Recent uplift of the Betic Cordillera, SE Spain. *Geomorphology*, **50**, 3–26.

Brolsma, M.J. 1975. Lithostratigraphy and foraminiferal assemblages of the Miocene-Pliocene transitional strata of Capo Rossello and Eraclea Minoa (Sicily, Italy). *Proceedings of the Koninklijke Nederlandse Akademie Van Wetenschappen*, Series B, **78**, 341–380.

Brolsma, M.J. 1976. Discussion on the arguments concerning the palaeoenvironmental interpretation of of the Arenazzolo in Capo Rossello and Eraclea Minoa (S. Sicily, Italy). *Memoria della Società geologica italiana*, **16**, 153–157.

Butler, R.W.H., Lickorish, W.H., Grasso, M., Pedley, H.M. and Ramberti, L. 1995. Tectonics and sequence stratigraphy in Messinian basins, Sicily: constraints on the initiation and termination of the Mediterranean salinity crisis. *Geological Society of America Bulletin*, **107**, 425–439.

Carnevale, G., Longinelli, A., Caputo, D., Barbieri, M. and Landini, W. 2008. Did the Mediterranean marine reflooding precede the Mio–Pliocene boundary? Paleontological and

geochemical evidence from upper Messinian sequences of Tuscany, Italy. *Palaeogeography, Palaeoclimatology, Palaeoecology*, **257**, 81–105, doi:10.1016/j.palaeo.2007.09.005

Catuneanu, O. and Zecchin, M. 2013. High-resolution sequence stratigraphy of clastic shelves II: controls on sequence development. *Marine and Petroleum Geology*, **39**, 26–38, http://dx.doi.org/10.1016/j.marpetgeo.2012.08.010

Cavazza, W. 1989. Detrital modes and provenance of the Stilo - Capo d'Orlando Formation (Miocene), southern Italy. *Sedimentology*, **36**, 1077–1090.

Cavazza, W. and Barone, M. 2010. Large-scale sedimentary recycling of tectonic mélange in a forearc setting: the Ionian basin (Oligocene-Quaternary, southern Italy). *Geological Society of America Bulletin*, **122**, 1932–11949, doi:10.1130/B30177.1

Cavazza, W., Blenkinsop, J., DeCelles, P., Patterson, R.T. and Reinhardt, E.D. 1997. Stratigrafia e sedimentologia della sequenza sedimentaria oligocenico-quaternaria del bacino calabro-ionico di avanarco. *Bollettino della Società geologica italiana*, **116**, 51–77.

Cavazza, W. and DeCelles, P.G. 1993. Miocene submarine canyons and associated sedimentary facies in southeastern Calabria, southern Italy. *Geological Society of America Bulletin*, **105**, 1297–1309.

Cavazza, W. and DeCelles, P.G. 1998. Upper Messinian siliciclastic rocks in southeastern Calabria (southern Italy): paleotectonic and eustatic implications for the evolution of the central Mediterranean region. *Tectonophysics*, **298**, 223–241.

Cavazza, W., Roure, F. and Ziegler, P.A. 2004. The Mediterranean area and the surrounding regions: active processes, remnants of former Tethyan oceans and related thrustbelts. *In*: Cavazza, W., Roure, F., Spakman, Stampfli, G.M. and Ziegler, P.A. (eds) *The TRANSMED Atlas: the Mediterranean Region from Crust to Mantle*. Springer-Verlag, 1–29.

Channell, J.E.T., Rio, D. and Thunell, R.C. 1988. Miocene/Pliocene boundary magnestostratigraphy at Capo Spartivento, Calabria, Italy. *Geology*, **16**, 1096–1099.

CIESM (Antón, J., Çağatay, M.N., De Lange, G., Flecker, R., Gaullier, V., Gunde- Cimerman, N., Hübscher, C., Krijgsman, W., Lambregts, P., Lofi, J., Lugli, S., Manzi, V., McGenity, T.J., Roveri, M., Sierro, F.J. and Suc, J.-P.) 2008. Executive Summary. *In*: Briand, F. (ed) *The Messinian Salinity Crisis from mega-deposits to microbiology – a Consensus Report*. *CIESM Workshop Monographs*, **33**, 7–28.

Cita, M.B. 1973. Inventory of biostratigraphical findings and problems. *In*: Ryan, W.B.F., Hsü, K.J. and Cita, M.B. (eds) *Initial Reports of the Deep Sea Drilling Project*, **13**, 2. U.S. Government Printing Office, Washington D.C., 1045–1073.

Cita, M.B., Wright, R.C., Ryan, W.B.F. and Longinelli, A. 1978. Messinian paleoenvironments. *In*: Hsü, K.J., Montadert, L. *et al*. (eds) *Initial Reports of the Deep Sea Drilling Project*, **42**, 1. U.S. Government Printing Office, Washington D.C., 1003–1035. doi:10.2973/dsdp.proc.42-1.153.1978

Clauzon, G., Suc, J.-P., Do Couto, D., Jouannic, G., Melinte-Dobrinescu, M.C., Jolivet, L., Quillévéré, F., Lebret, N., Mocochain, L., Popescu, S.-M., Martinell, J., Doménech, R., Rubino, J.-L., Gumiaux, C., Warny, S., Bellas, S.M., Gorini, C., Bache, F., Rabineau, M. and Estrada, F. 2015. New insights on the Sorbas Basin (SE Spain): the onshore reference of the Messinian Salinity Crisis. *Marine and Petroleum Geology*, **66**, 71–100, http://dx.doi.org/10.1016/j.marpetgeo.2015.02.016

Clauzon, G., Suc, J.-P., Popescu, S.-M., Marunteanu, M., Rubino, J.-L., Marinescu, F. and Melinte, M.C. 2005. Influence of the Mediterranean sea-level changes over the Dacic Basin (Eastern Paratethys) in the Late Neogene. The Mediterranean Lago Mare facies deciphered. *Basin Research*, **17**, 437–462, doi: 10.1111/j.1365-2117.2005.00269.x

Clauzon, G., Suc, J.-P., Gautier, F., Berger, A. and Loutre, M.-F. 1996. Alternate interpretation of the Messinian salinity crisis: controversy resolved? *Geology*, **24**, 363–366.

Cohen, K.M., Finney, S.C., Gibbard, P.L. and Fan, J.-X. 2020. International Chronostratigraphic Chart, http://www.stratigraphy.org/ICSchart/ChronostratChart2020-03.pdf

Cornée, J.-J., Ferrandini, M., Saint Martin, J.P., Münch, P., Moullade, M., Ribaud-Laurenti, A., Roger, S., Saint Martin, S. and Ferrandini, J. 2006. The late Messinian erosional surface and the subsequent reflooding in the Mediterranean: new insights from the Melilla–Nador basin (Morocco). *Palaeogeography, Palaeoclimatology, Palaeoecology*, **230**, 129–154, doi:10.1016/j.palaeo.2005.07.011

Critelli, S., Muto, F. and Tripodi, V. 2015a. Geological Map of Italy, 1:50,000 scale, sheet **630** Bovalino. Geological Survey of Italy, Rome.

Critelli, S., Muto, F. and Tripodi, V. 2015b. Geological Map of Italy, 1:50,000 scale, sheet **590** Taurianova. Geological Survey of Italy, Rome.

De Astis, G., Ventura, G. and Vilardo, G. 2003. Geodynamic significance of the Aeolian volcanism (southern Tyrrhenian Sea, Italy) in light of structural, seismological, and geochemical data. *Tectonics*, **22**, 1040–1057, doi: 10.1029/2003TC001506

DeCelles, P.G. and Cavazza, W. 1992. Constraints on the formation of Pliocene hummocky cross-stratification in Calabria (southern Italy) from consideration of hydraulic and dispersive equivalence, grain-flow theory and suspended-load fallout rate. *Journal of Sedimentary Petrology*, **62**, 555–568.

DeCelles, P. and Cavazza, W. 1995. Upper Messinian fanglomerates in eastern Calabria (southern Italy): response to microplate migration and Mediterranean sea-level changes. *Geology*, **23**, 775–778.

Decima, A. 1964. Ostracodi del genere *Cyprideis* Jones del Neogene e del Quaternario italiani. *Palaeontographia italica*, **57**, 81–133.

Decima, A., Mckenzie, J.A. and Schreiber, B.C. 1988. The origin of "evaporative" limestones: an example from the Messinian of Sicily (Italy). *Journal of Sedimentary Petrology*, **58**, 256–272.

Decima, A. and Wezel, F.C. 1973. Late Miocene evaporites of the central Sicilian Basin. *In*: Ryan, W.B.F., Hsü, K.J. and Cita, M.B. (eds) *Initial Reports of the Deep Sea Drilling Project*, **13**, 2. U.S. Government Printing Office, Washington D.C., 1234–1241.

Dercourt, J., Zobebshain, L.P., Ricou, M.-E., Kazmin, V.G., Le Pichon, X., Knipper, A.L., Grandjacquet, C., Sborshchikov, I.M., Boulin, J., Sorokhtin, O., Geyssant, J., Lepvrier, C., Biju-Duval, B., Sibuet, J.-C., Savostin, L.A., Westphal, M. and Lauer, J.-P. 1985. Présentation de 9 cartes paléogéographiques au 1/20.000.000^{e} s'étendant de l'Atlantique au Pamir pour la période du Lias à l'Actuel. *Bulletin de la Société géologique de France*, Series 8, **1**, 5, 637–652.

Dewey, J.F., Helman, M.L., Turco, E., Hutton, D.W.H. and Knott, S.D. 1989. Kinematics of the Western Mediterranean. *In*: Coward, M.P., Dietrich, D. and Park, G. (eds) *Alpine Tectonics*. *Geological Society of London, Special Publication*, **45**, 265–283.

Do Couto, D., Popescu, S.-M., Suc, J.-P., Melinte-Dobrinescu, M.C., Barhoun, N., Gorini, C., Jolivet, L., Poort, J., Jouannic, G. and Auxietre, J.-L. 2014. Lago Mare and the Messinian Salinity Crisis: evidences from the Alboran Sea (S. Spain). *Marine and Petroleum Geology*, **52**, 57-76, http://dx.doi.org/10.1016/j.marpetgeo.2014.01.018

Dondi, L. 1985. Pianura Padana: paleogeografia dall'Oligocene superior al Pleistocene. *Atti del Convegno Regionale di Cartografia di Bologna*, 1985, Regione Emilia–Romagna, 76–101.

El Euch-El Koundi, N., Ferry, S., Suc, J.-P., Clauzon, G., Melinte-Dobrinescu, M.C., Gorini, C., Safra, A. and Zargouni, F. 2009. Messinian deposits and erosion in northern Tunisia: inferences on Strait of Sicily during the Messinian Salinity Crisis. *Terra Nova*, **21**, 41–48, doi: 10.1111/j.1365-3121.2008.00852.x

Fabri, A. and Curzi, P. 1979. The Messinian of the Tyrrhenian Sea: seismic evidence and dynamic implications. *Giornale di Geologia*, **43**, 215–248.

Gautier, F., Clauzon, G., Suc, J.-P., Cravatte, J. and Violanti, D. 1994. Age et durée de la crise de salinité messinienne. *Comptes-Rendus de l'Académie des Sciences de Paris*, **318**, ser. 2, 1103–1109.

Gorini, C., Haq, B.U., Reis, A.T., dos, Silva, C.G., Cruz, A., Soares, E. and Grangeon, D. 2014. Late Neogene sequence stratigraphic evolution of the Foz do Amazonas Basin, Brazil. *Terra*

Nova, **26**, 179–185, doi: 10.1111/ter.12083
Gueguen, E., Doglioni, C. and Fernandez, M. 1998. On the post-25 Ma geodynamic evolution of the western Mediterranean. *Tectonophysics*, **298**, 259–269.
Guido, A., Jacob, J., Gautret, P., Laggoum-Défarge, Mastandrea, A. and Russo, F. 2007. Molecular fossils and other organic markers as palaeoenvironmental indicators of the Messinian Calcare di base Formation: normal *versus* stressed marine deposition (Rossano Basin, northern Calabria, Italy). *Palaeogeography*, *Palaeoclimatology*, *Palaeoecology*, **255**, 265–283, doi:10.1016/j.palaeo.2007.07.015
Haq, B., Gorini, C., Baur, J., Moneron, J. and Rubino, J.-L. 2020. Deep Mediterranean's Messinian evaporite giant: how much salt? *Global and Planetary Change*, 184, 103052, https://doi.org/10.1016/j.gloplacha.2019.103052
Henriquet, M., Dominguez, S., Barreca, G., Malavieille, J., and Monaco, C. 2020. Structural and tectono-stratigraphic review of the Sicilian orogen and new insights from analogue modeling. Earth-Science Reviews, **208**, 103257, https://doi.org/10.1016/j.earscirev.2020.103257
Hilgen, F.J. 1987. Sedimentary rhythms and high-resolution chronostratigraphic correlations in the Mediterranean Pliocene. *Newsletters on Stratigraphy*, 17, 109–127, doi: 10.1127/nos/17/1987/109
Hilgen, F.J. 1991. Extension of the astronomically calibrated (polarity) time scale to the Miocene/Pliocene boundary. *Earth and Planetary Science Letters*, **107**, 349–368.
Hilgen, F.J. and Langereis, C.G. 1993. A critical re-evaluation of the Miocene/Pliocene boundary as defined in the Mediterranean. *Earth and Planetary Science Letters*, **118**, 167–179.
Hilgen, F.J., Lourens, L.J. and Van Dam, J.A. 2012. The Neogene Period. *In*: Gradstein, F., Ogg, J., Schmitz, M. and Ogg, G. (eds), *The Geological Time Scale 2012*, 1, 29. Elsevier, 923–978.
Hsü, K.J. 1972. Origin of Saline Giants: a critical review after the discovery of the Mediterranean evaporite. *Earth-Science Reviews*, **8**, 371–396.
Hsü, K.J., Cita, M.B. and Ryan, W.B.F. 1973a. The origin of the Mediterranean evaporites. *In*: Ryan, W.B.F., Hsü, K.J. and Cita, M.B. (eds) *Initial Reports of the Deep Sea Drilling Project*, **13**, 2. U.S. Government Printing Office, Washington D.C., 1203–1231, doi:10.2973/dsdp.proc.13.143.1973
Hsü, K.J., Ryan, W.B.F. and Cita, M. 1973*b*. Late Miocene desiccation of the Mediterranean. *Nature*, **242**, 240–244.
Iaccarino, S. and Bossio, A. 1999. Paleoenvironment of uppermost Messinien sequences in the Western Mediterranean (Sites 974, 975, and 978). *In*: Zahn, R., Comas, M.C. and Klaus, A. (eds) *Proceedings of the Ocean Drilling Program*, *Scientific Results*, **161**, College Station, TX (Ocean Drilling Program), 529–541, doi:10.2973/odp.proc.sr.161.246.1999.
Iaccarino, S.M. and Premoli Silva, I. 2007. Practical manual of Neogene planktonic foraminifera. *In*: Biolzi, M., Iaccarino, S.M., Turco, E., Checconi, A. and Rettori, R. (eds) *International school on planktonic foraminifera*. Università degli Studi di Perugia, 1–142.
Jolivet, L., Augier, R., Robin, C., Suc, J.-P. and Rouchy, J.M. 2006. Lithospheric-scale geodynamic context of the Messinian salinity crisis. *Sedimentary Geology*, **188–189**, 9–33, doi:10.1016/j.sedgeo.2006.02.004
Jolivet, L. and Faccenna, C. 2000. Mediterranean extension and the Africa-Eurasia collision. *Tectonics*, **19**, 1095–1106.
Karakitsios, V., Roveri, M., Lugli, S., Manzi, V., Gennari, R., Antonarakou, A., Triantaphyllou, M., Agiadi, K., Kontakiotis, G., Kafousia, N. and de Rafelis, M. 2017. A record of the Messinian salinity crisis in the eastern Ionian tectonically active domain (Greece, eastern Mediterranean). *Basin Research*, **29**, 203–233, doi:10.111/bre.12173
Kastens, K.A., Mascle, J., Auroux, C., Bonatti, E., Broglia, C., Channell, J., Curzi, P., Emeis, K.-C., Glaçon, G., Hasegawa, S., Hieke, W., McCoy, F., Mckenzie, J., Mascle, G., Mendelson, J., Müller, C., Réhault, J.-P., Robertson, A., Sartori, R., Sprovieri, R. and Torii, M. (eds) 1990. *Tyrrhenian Sea, Proceedings of the Ocean Drilling Program*, Scientific Results, **107**, doi:10.2973/odp.proc.sr.107.1990

Krijgsman, W., Capella, W., Simon, D., Hilgen, F.J., Kouwenhoven, T.J., Meijer, P.Th., Sierro, F.J., Tulbure, M.A., van den Berg, B.C.J., van der Schee, M. and Flecker, R. 2018. The Gibraltar Corridor: Watergate of the Messinian Salinity Crisis. *Marine Geology*, **403**, 238–246, https://doi.org/10.1016/j.margeo.2018.06.008

Krijgsman, W., Fortuin, A.R., Hilgen, F.J. and Sierro, F.J. 2001. Astrochronology for the Messinian Sorbas basin (SE Spain) and orbital (precessional) forcing for evaporite cyclicity. *Sedimentary Geology*, **140**, 43–60.

Krijgsman, W., Hilgen, F.J., Raffi, I., Sierro, F.J. and Wilson, D.S. 1999. Chronology, causes and progression of the Messinian salinity crisis. *Nature*, **400**, 652–655,

Lirer, F., Foresi, L.M., Iaccarino, S.M., Salvatorini, G., Turco, E., Cosentino, C., Sierro, F.J. and Caruso, A. 2019. Mediterranean Neogene planktonic foraminifer biozonation and biochronology *Earth-Science Reviews*, **196**, 102869, https://doi.org/10.1016/j.earscirev.2019.05.013

Londeix, L., Benzakour, M., Suc, J.-P. and Turon J.-L. 2007. Messinian palaeoenvironments and hydrology in Sicily (Italy): the dinoflagellate cyst record. *Geobios*, **40**, 233–250, doi:10.1016/j.geobios.2006.12.001

Malinverno, A. and Ryan, W.B.F. 1986. Extension in the Tyrrhenian Sea and shortening in the Apennines as result of arc migration driven by sinking of the lithosphere. *Tectonics*, **5**, 227–245.

Maniscalco, R., Casciano, C.I., Distefano, S., Grossi, F., and Di Stefano, A. 2019. Facies analysis in the Second Cycle Messinian evaporates predating the early Pliocene reflooding: the Balza Soletta secion (Corvillo Basin, central Sicily). *Italian Journal of Geosciences*, **138**, 301–316, https://doi.org/10.3301/IJG.2019.06

Manzi, V., Argnani, A., Corcagnani, A., Lugli, S. and Roveri, M. 2020. The Messinian salinity crisis in the Adriatic foredeep: evolution of the largest evaporitic marginal basin in the Mediterranean. *Marine and Petroleum Geology*, **115**, 104288, https://doi.org/10.1016/j.marpetgeo.2020.104288

Manzi, V., Gennari, R., Hilgen, F., Krijgsman, W., Lugli, S., Roveri, M. and Sierro, F.J. 2013. Age refinement of the Messinian salinity crisis onset in the Mediterranean. *Terra Nova*, **25**, 315–322, doi: 10.1111/ter.12038

Manzi, V., Lugli, S., Roveri, M., Schreibern B.C. and Gennari, R. 2011. The Messinian "Calcare di Base" (Sicily, Italy) revisited. *Geological Society of America Bulletin*, **123**, 347–370, doi: 10.1130/B30262.1

Melinte-Dobrinescu, M.C., Suc, J.-P., Clauzon, G., Popescu, S.-M., Armijo, R., Meyer, B., Biltekin, D., Çağatay, M.N., Ucarkus, G., Jouannic, G., Fauquette, S. and Çakir, Z. 2009. The Messinian Salinity Crisis in the Dardanelles region. Chronostratigraphic constraints. *Palaeogeography, Palaeoclimatology, Palaeoecology*, **278**, 24–39, doi:10.1016/j.palaeo.2009.04.009

Micallef, A., Camerlenghi, A., Georgiopoulou, A., Garcia-Castellanos, D., Gutscher, M.-A., Lo Iacono, C., Huvenne, V.A.I., Mountjoy, J.J., Paull, C.K., Le Bas, T., Spatola, D., Facchin, L. and Accettella, D. 2019. Geomorphic evolution of the Malta Escarpment and implications for the Messinian evaporative drawdown in the eastern Mediterranean Sea. *Geomorphology*, **327**, 264 – 283, https://doi.org/10.1016/j.geomorph.2018.11.012

Miller, K.G., Mountain, G.S., Wright, J.D. and Browning, J.V. 2011. A 180-million-year record of sea level and ice volume cariations from continental margin and deep-sea isotopic records. *Oceanography*, **24**, 2, 40–53.

Montadert, L., Sancho, J., Fail, J.P., Debyser, J. and Winnock, E. 1970. De l'âge tertiaire de la série salifère responsable des structures diapiriques en Méditerranée Occidentale (Nord-Est des Baléares). *Comptes Rendus de l'Académie des Sciences de Paris*, **271**, 812–815.

Ogniben, L. 1957. Petrografia della Serie Solfifera Siciliana e considerazioni geologiche relative. *Memorie Descrittive della Carta Geologica d'Italia*, **33**, 1–275.

Patterson, R.T., Blenkinsop, J. and Cavazza, W. 1995. Planktic foraminiferal biostratigraphy and $^{87}Sr/^{86}Sr$ isotopic stratigraphy of the Oligocene-to-Pleistocene sedimentary sequence in the southeastern Calabrian microplate, southern Italy. *Journal of Paleontology*, **69**, 7–20.

Pellen, R., Popescu, S.-M., Suc, J.-P., Melinte-Dobrinescu, M C., Rubino, J.-L-, Rabineau, M., Marabini, S., Loget, N., Casero, P., Cavazza, W., Head, M. and Aslanian, D. 2017. The Apennine foredeep (Italy) during the latest Messinian: Lago Mare reflects competing brackish and marine conditions based on calcareous nannofossils and dinoflagellate cysts. *Geobios*, **50**, 237–257, http://dx.doi.org/10.1016/j.geobios.2017.04.004

Perch-Nielsen, K. 1985. Cenozoic calcareous nannofossils. *In*: Bolli, H.M., Saunders, J.B. and Perch-Nielsen, K. (eds) *Plankton Stratigraphy*. Cambridge University Press, 427–554.

Popescu, S.-M., Dalesme, F., Jouannic, G., Escarguel, G., Head, M.J., Melinte-Dobrinescu, M.C., Sütő-Szentai, M., Bakrac, K., Clauzon, G. and Suc, J.-P. 2009. *Galeacysta etrusca* complex, dinoflagellate cyst marker of Paratethyan influxes into the Mediterranean Sea before and after the peak of the Messinian Salinity Crisis. *Palynology*, **33**, 105–134.

Popescu, S.-M., Dalibard, M., Suc, J.-P., Barhoun, N., Melinte-Dobrinescu, M.C., Bassetti, M.A., Deaconu, F., Head, M.J., Gorini, C., Do Couto, D., Rubino, J.-L., Auxietre, J.-L. and Floodpage, J. 2015. Lago Mare episodes around the Messinian-Zanclean boundary in the deep southwestern Mediterranean. *Marine and Petroleum Geology*, **66**, 55–70, http://dx.doi.org/10.1016/j.marpetgeo.2015.04.002

Raffi, I., Backman, J., Fornaciari, E., Pälike, H., Rio, D., Lourens, L. and Hilgen, F. 2006. A review of calcareous nannofossil astrobiochronology en compassing the past 25 million years. *Quaternary Science Reviews*, **25**, 3113–3137, doi:10.1016/j.quascirev.2006.07.007

Riding, R., Braga, J.C., Martín, J.M. and Sánchez-Almazo, I. 1998. Mediterranean Messinian Salinity Crisis: constraints from a coeval marginal basin, Sorbas, southeastern Spain. *Marine Geology*, **146**, 1–20.

Roveri, M., Flecker, R., Krijgsman, W., Lofi, J., Lugli, S., Manzi, V., Sierro, F.J., Bertini, A., Camerlenghi, A., De Lange, G., Govers, R., Hilgen, F.J., Hübscher, C., Meijer, P.Th. and Stoica, M. 2014. The Messinian Salinity Crisis: past and future of a great challenge for marine sciences. *Marine Geology*, **352**, 25–50, http://dx/doi.org/10.1016/j.margeo.2014.02.002

Ruggieri, G. 1967. The Miocene and later evolution of the Mediterranean Sea. *In*: Adams, C.G., and Ager, A.V. (eds) *Aspects of Tethyan Biogeography*, 7. S*ystematics Association, Special Publications*, 283–290.

Ryan, W.B.F. 2009. Decoding the Mediterranean salinity crisis. *Sedimentology*, **56**, 95–136, doi:101111/j.1365-3091-2008.01031.x

Selli, R. 1954. Il Bacino del Metauro. *Giornale di Geologia*, **24**, 1–294.

Selli, R. 1960. Il Messiniano Mayer-Eymar 1867. Proposta di un neostratotipo. *Giornale di Geologia*, **28**, 1–33.

Soria, J.M., Caracuel, J.E., Corbí, H., Dinarès-Turell, J., Lancis, C., Tent-Manclús, J.E. and Yébenes, A. 2008. The Bajo Segura Basin (SE Spain): implications for the Messinian salinity crisis in the Mediterranean margins. *Stratigraphy*, **5**, 257–263.

Spakman, W. and Wortel, R. 2004. A tomographic view on western Mediterranean geodynamics. *In*: Cavazza, W., Roure, F., Spakman, W., Stampfli, G.M. and Ziegler, P.A. (eds) *The TRANSMED Atlas: the Mediterranean Region from Crust to Mantle*. Springer-Verlag, 31–52.

Sternai, P., Caricchi, L., Garcia-Castellanos, D., Jolivet, L., Sheldrake, T.E. and Castelltort, S. 2017. Magmatic pulse driven by sea-level changes associated with the Messinian salinity crisis. *Nature Geoscience*, **10**, 783–787, https://doi.10.1038/NGEO3032

Suc, J.-P., Bache, F., Çağatay, M.N. and Csato, I. 2015. Messinian events and hydrocarbon exploration in the Mediterranean: an introduction. *Marine and Petroleum Geology*, **66**, 1–5, http://dx.doi.org/10.1016/j.marpetgeo.2015.05.006

Thunnell, R.C., Williams, D.F. and Howell, M. 1987. Atlantic-Mediterranean water exchange during the late Neogene. *Paleoceanography*, **2**, 661–678.

Tortorici, D.L., Monaco, C., Tansi, C. and Cocina, O. 1995. Recent and active tectonics in the Calabrian arc (Southern Italy). *Tectonophysics*, **243**, 37–55.

Vai, G.B. and Ricci-Lucchi, F. 1977. Algal crusts, autochtonous and clastic gypsum in a cannibalistic evaporite basin: a case history from the Messinian of northern Apennines. *Sedimentology*, **24**, 211–244.

Van Couvering, J.A., Castradori, D., Cita, M.B., Hilgen, F.J. and Rio, D. 2000. The base of the Zanclean Stage and of the Pliocene Series. *Episodes*, **23**, 3, 179–187.

Van Dijk, J.P. 1992. *Late Neogene fore-arc basin evolution in the Calabrian Arc (central Mediterranean): tectonic sequence stratigraphy and dynamic geohistory*. PhD thesis, University of Utrecht.

Williams, G.L., Fensome, R.A. and MacRae, R.A. 2017. DINOFLAJ3, American Association of Stratigraphic Palynologists, Data Series no. 2, http://dinoflaj.smu.ca/dinoflaj3

Young, J.R. 1998. Chapter 8: Neogene. *In* : Bown, P.R. (ed) *Calcareous Nannofossils Biostratigraphy*. British Micropaleontological Society Publications Series. Kluwer Academic Press, 225–265.

Zeeden, C., Hilgen, F., Westerhold, T., Lourens, L., Röhl, U. and Bickert, T. 2013. Revised Miocene splice, astronomical tuning and calcareous plankton biochronology of ODP Site 926 between 5 and 14.4 Ma. *Palaeogeography, Palaeoclimatology, Palaeoecology*, **369**, 430–451, http://dx.doi.org/10.1016/j.palaeo.2012.11.009

Zijderveld, J.D.A., Zachariasse, W.J., Verhallen, P.J.J.M. and Hilgen, F.J. 1986. The age of the Miocene–Pliocene boundary. *Newsletters on Stratigraphy*, **16**, 169–181.

Table 1. *Information on the six sampled locations*

Region	Location	Latitude N	Longitude E	Altitude (m)	Number of samples
Guardavalle	G3	38°30’28.97”	16°30’09.42”	265	3
	G5	38°28’38.79”	16°30’47.08”	110	2
Caulonia	A2	38°23’52.95”	16°26’07.12”	266	3
	A4	38°23’11.50”	16°26’11.70”	167	1
	C4	38°22’20.10”	16°25’18.60”	167	6
Careri		38°10’56.30”	16°06’56.00”	400	2

Table 2. *Occurrence of the calcareous nannofossils by location and sample.*

Region	Guardavalle					Caulonia										Careri	
Location	G3			G5		A2			A4	C4							
Samples	1	2	3	1	2	1	2	3	1	1	2	3	4	5	6	1	2
Amaurolithus delicatus	x		x									x				x	x
Amaurolithus primus	x	x		x	x	x			x		x					x	
Calcidiscus leptoporus	x	x	x	x	x	x	x	x	x	x	x	x	x	x	x	x	x
Calcidiscus macintyrei	x	x	x	x	x	x	x	x	x	x	x	x	x	x	x	x	x
Ceratolithus acutus				x	x						x	x					
Coccolithus pelagicus	x	x	x	x	x	x	x	x	x	x	x	x	x	x	x	x	x
Discoaster asymmetricus				x	x						x	x		x	x		x
Discoaster berggrenii	x	x	x		x	x					x	x		x	x	x	x
Discoaster brouweri	x	x	x	x	x	x		x	x	x	x	x	x	x	x	x	x
Discoaster quinqueramus	x	x	x			x										x	
Discoaster surculus	x	x	x			x			x							x	x
Helicosphaera carteri	x	x	x	x	x	x	x	x	x	x	x	x	x	x	x	x	x
Helicosphaera sellii				x	x			x		x	x	x	x	x	x		x
Nicklithus amplificus			x													x	
Orthorhabdus rugosus	x	x				x	x									x	
Pontosphaera japonica	x	x	x	x	x	x	x	x	x	x	x	x	x	x	x	x	x
Pontosphaera multipora					x		x				x	x		x	x		
Reticulofenestra haquii	x	x	x	x	x	x	x	x	x	x	x	x	x	x	x	x	x
Reticulofenestra minuta	x	x	x	x	x	x	x	x	x	x	x	x	x	x	x	x	x
Reticulofenestra minutula	x	x	x	x	x	x	x	x	x	x	x	x	x	x	x	x	x
Reticulofenestra pseudoumbilicus	x	x	x	x	x	x	x	x	x	x	x	x	x	x	x	x	x
Rhabdosphaera clavigera	x	x	x			x										x	
Scyphosphaera spp.						x										x	
Sphenolithus abies	x	x	x				x	x		x			x				
Syracosphaera spp.		x	x			x										x	
Thoracosphaera spp.																	x
Reworked specimens	x	x	x	x	x	x	x	x	x	x	x	x	x	x	x	x	x

x = present

1 Sample from the Trubi Formation

1 Sample from Unit 3

Table 3. *Occurrence of the planktonic foraminifera by location and sample. The three samples come from the Trubi Formation.*

Region	**Caulonia**		**Careri**
Location	A2		
Samples	2	3	2
Globigerina bulloides	x	x	x
Globigerina falconensis			x
Globigerinella obesa	x		x
Globigerinella siphonifera			x
Globigerinita glutinata			x
Globigerinita uvula			x
Globigerinoides bollii			x
Globigerinoides extremus	x	x	x
Globigerinoides quadrilobatus			x
Globigerinoides sacculifer			x
Globigerinoides trilobus	x		x
Globorotalia aff. *margaritae*			x
Globorotalia scitula	x		x
Globoturborotalita apertura		x	
Globoturborotalita decoraperta	x	x	x
Neogloboquadrina acostaensis sinistral	x		
Neogloboquadrina acostaensis dextral			x
Orbulina universa	x	x	x
Sphaeroidinellopsis seminulina	x		x

x = present

Table 4. *Results of the dinoflagellate cyst analyses detailed by location and sample, including the suggested paleoenvironment.*
Environment: coastal to lagoonal species are written in a light grey box; coastal species in a dark grey box; open marine species in a black box.

Region	**Caulonia**					
Location	C4					A4
Samples	1	2	4	5	6	1
Achomosphaera andalousiensis						1
Brigantedinium sp.		1				
Cyst of *Pentapharsodinium dalei*			1		1	
Edwardsiella sexispinosa			1			
Homotryblium sp.			7		4	22
Hystrichokolpoma sp.			1			
Hystrichokolpoma rigaudiae			1			1
Impagidinium aculeatum					7	1
Impagidinium patulum	2		13	9	80	2
Impagidinium sp.			1	2	6	2
Impagidinium sphaericum				1	20	
Impagidinium strialatum						1
Invertocysta tabulata			1	1		1
Lingulodinium machaerophorum	1		12	2	10	67
Melitasphaeridium choanophorum			3		2	3
Nematosphaeropsis labyrinthus				1	2	
Nematosphaeropsis lattivitatus					6	
Operculodinium centrocarpum		1	4	1	2	7
Operculodinium janduchenei			3	1	8	6
Polysphaeridium zoharyi			1			2
Quinquecuspis concreta						1
Reticulatosphaera actinocoronata					1	1
Selenopemphix nephroides						7
Spiniferites bulloideus						1
Spiniferites falcipedius			1			
Spiniferites hyperacanthus			1			1
Spiniferites mirabilis	1		1			
Spiniferites ramosus			1	1		3
Spiniferites sp. (marine)			2	2		7
Reworked individuals			5	3		11

1 Sample from Unit 3

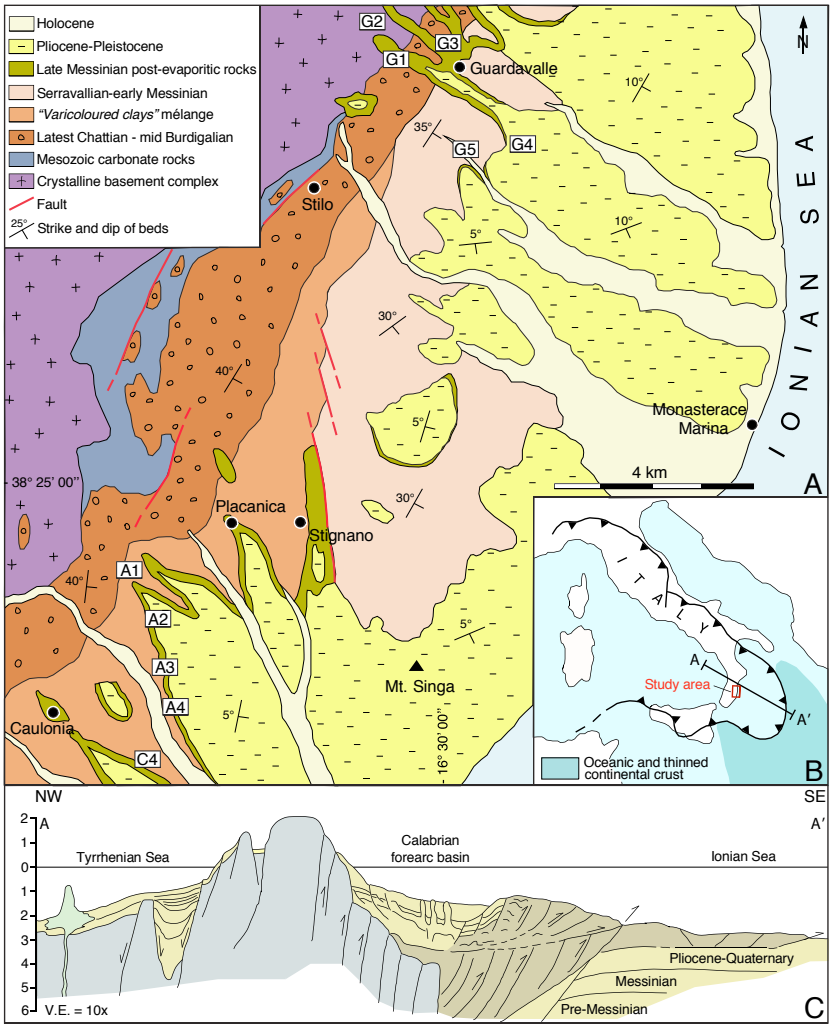

Fig. 1. (**A**) Simplified geologic map of the study area (after Cavazza and DeCelles 1998). Explanation of symbols: 1 = strike and dip of beds; 2 = faults; 3 = crystalline basement complex; 4 = Mesozoic carbonate rocks; 5 = latest Chattian–middle Burdigalian; 6 = "*Varicoloured clays*" mélange; 7 = Serravallian–early Messinian; 8 = late Messinian post-evaporitic rocks (units 2 and 3; Fig. 2); 9 = Pliocene–Pleistocene (cyclic whitish-grey calcilutites), 10 = Holocene (pebbles in fluvial terraces, sandstones on beaches). Labels indicate location of stratigraphic sections shown in Figures 5 and 6. (**B**) Present-day geodynamic sketch of the central Mediterranean region. **(C)** Structural cross-section across the Calabrian orogenic wedge and forearc basin (from Van Dijk 1992, modified). See (B) for location of cross-section.

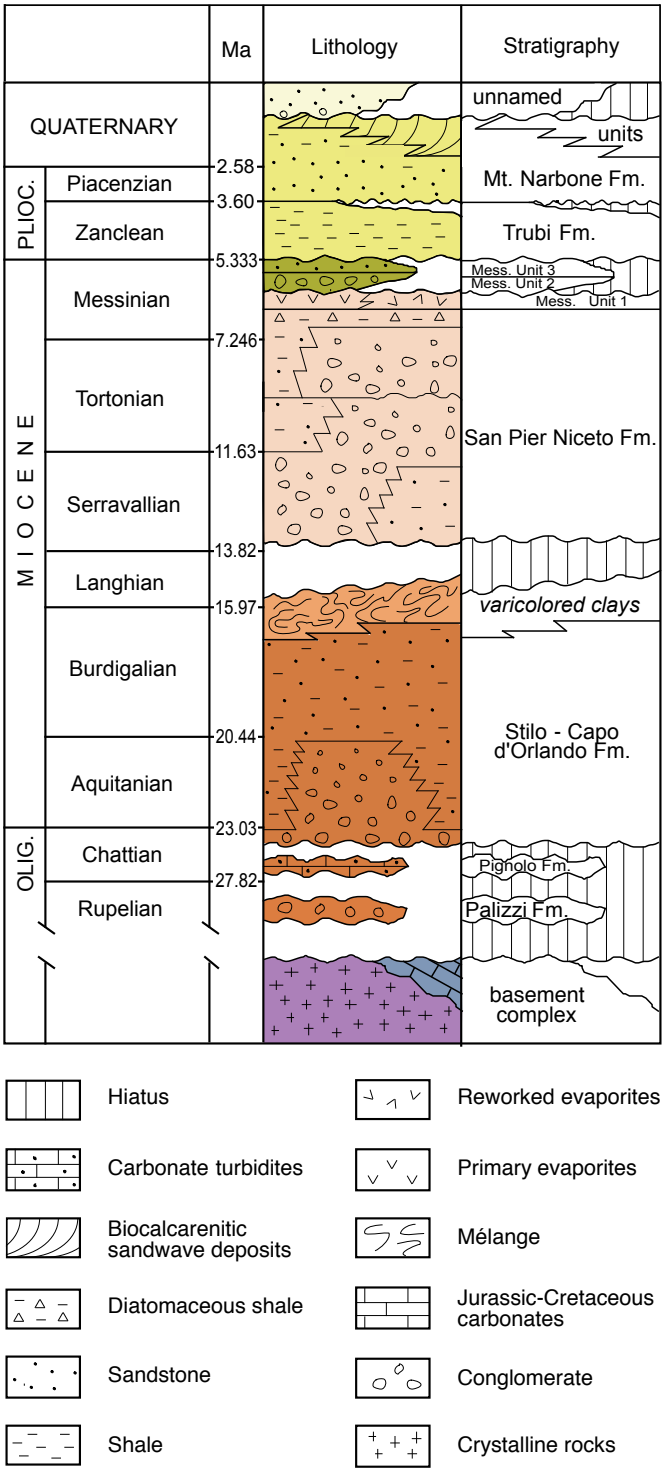

Fig. 2. Chronolithostratigraphy of the Ionian forearc-basin fill in southeastern Calabria. Sources: DeCelles and Cavazza (1992, 1995); Cavazza and DeCelles (1993, 1998); Patterson *et al*. (1995); Cavazza *et al*. (1997); Bonardi *et al*. (2001), Cavazza and Barone (2010) and unpublished data. Time scale after Cohen *et al*. (2020).

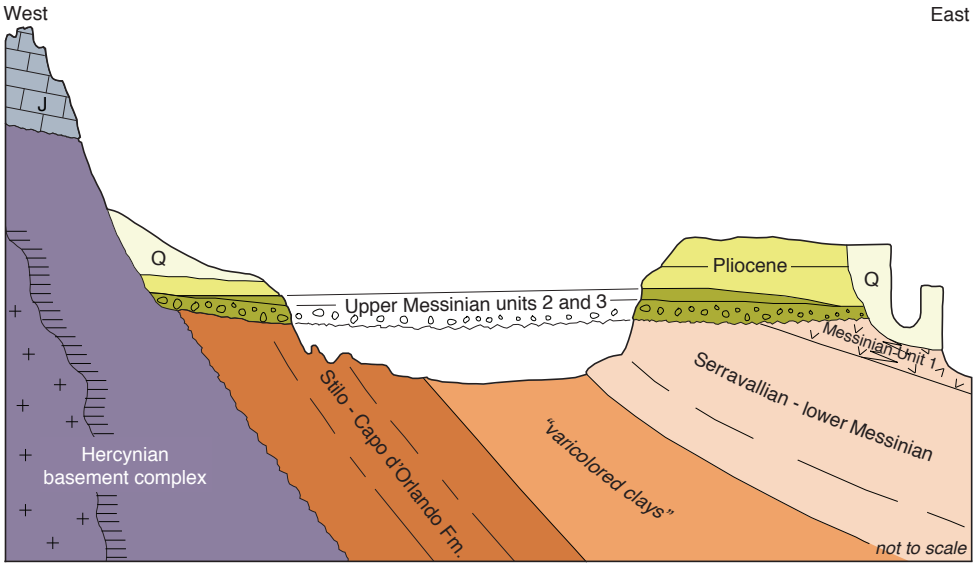

Fig. 3. Overall geometric relationships among the various lithostratigraphic units cropping out in the study area. The sketch is not to be intended as an actual geological section across any given area but as a broad depiction of the geometric relationships valid over the entire region. Note the sharp intra-Messinian angular unconformity between the early Messinian evaporites (Unit 1) and the overlying late Messinian post-evaporitic fanglomerates (Unit 2) and sandstone-dominated coastal deposits (Unit 3). Messinian Unit 3 pinches out both toward the continent and the Ionian Basin, thus defining a sedimentary prism (see text for further details), and it is overlain by the Early Pliocene Trubi Formation.

Fig. 4. The intra-Messinian unconformity at Careri. Messinian evaporite beds of Unit 1 (dashed lines) are unconformably overlain by subhorizontal fanglomerate beds of upper Messinian Unit 2.

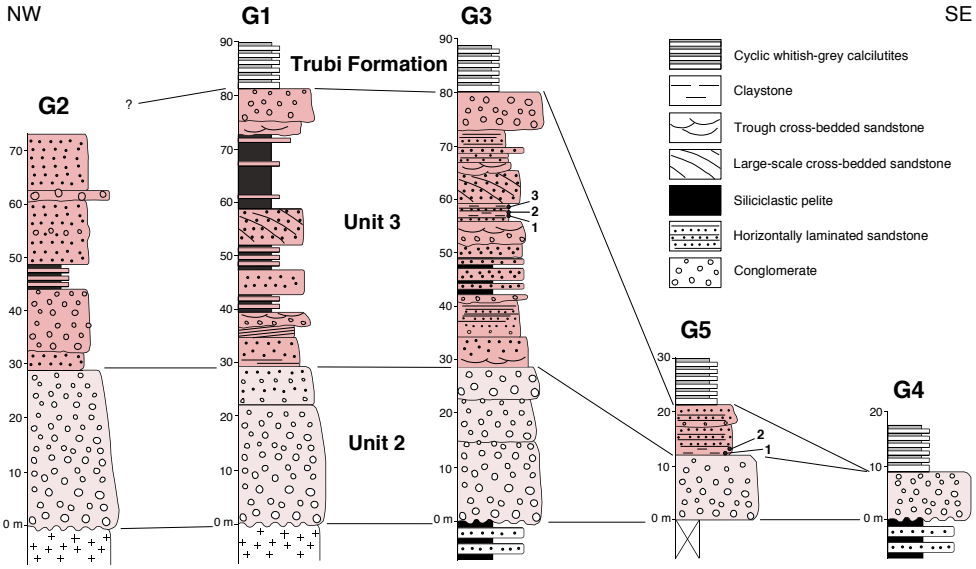

Fig. 5. Stratigraphic diagram of the upper Messinian post-evaporitic units of the Guardavalle region. G1 to G5 are the studied sections with the number and place of the analysed samples indicated by black dots (see Figure 1 for location). Evaporites (Unit 1 of Figures 2 and 3) are absent in this region. Coarse-grained upper Messinian fanglomerates (Unit 2) overlie unconformably either the crystalline basement complex (columns G1 and G2) or sedimentary deposits of Serravallian-Tortonian age (columns G3 and G4). Upper Messinian shallow marine to transitional deposits of Unit 3 define a sedimentary prism pinching out toward the southeast. Columns G1-4 after Cavazza and DeCelles (1998).

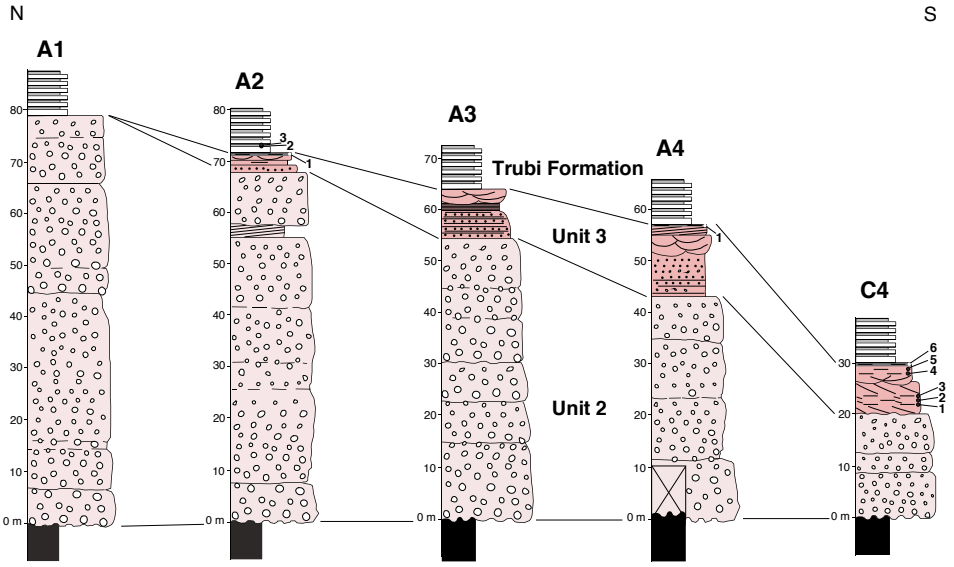

Fig. 6. Stratigraphic diagram of the upper Messinian post-evaporitic units of the Caulonia region. A1 to A4 and C4 are the studied sections with the number and place of the analysed samples indicated by black and white dots (see Figure 1 for location). Same legend as Figure 5. Evaporites (Unit 1 of Figures 2 and 3) are absent in this region. Coarse-grained upper Messinian fanglomerates (Unit 2) overlie erosively the pelitic mélange of the *Varicoloured clays* (see Fig. 3) Upper Messinian shallow marine to transitional deposits of Unit 3 define a sedimentary prism pinching out toward the northwest. Columns A1-3 after Cavazza and DeCelles (1998).

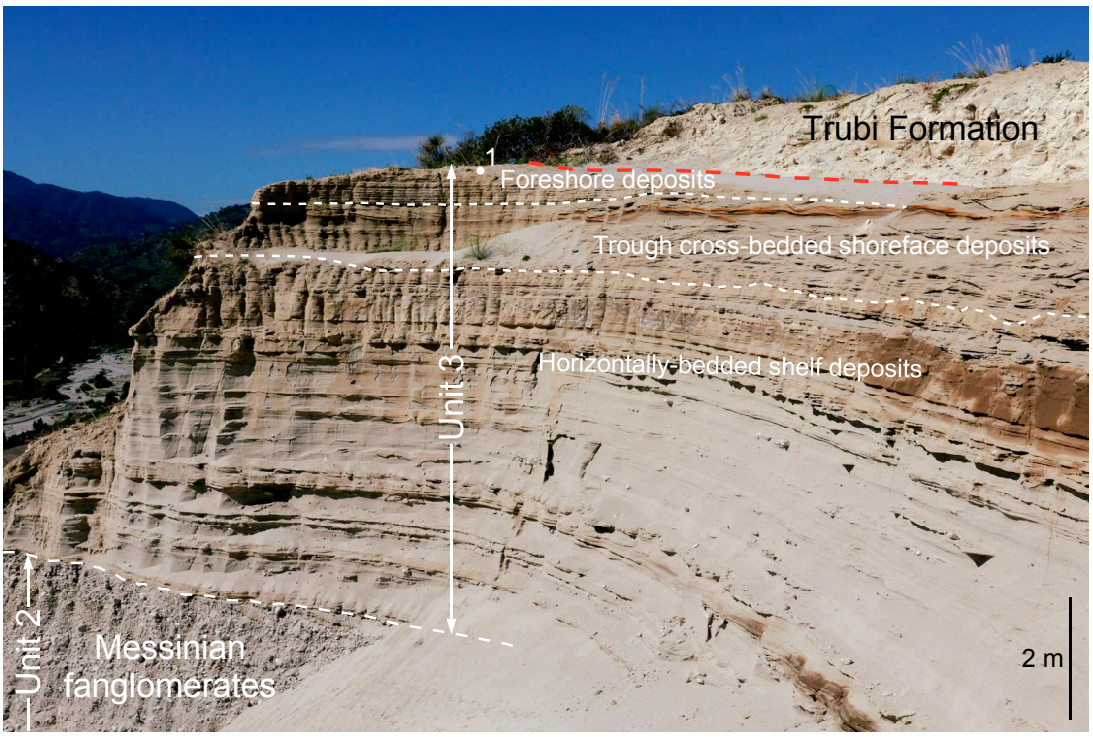

Fig. 7. Photograph of the upper part of section A4 (see Figures 1 and 5 for location) showing the topmost Unit 2, the entire Unit 3 and the lowermost Trubi Formation. White dot: studied sample. Upper Messinian Unit 3 forms a progradational parasequence from horizontally bedded shelfs deposits (very coarse sandstone with microconglomerate stringers) through trough cross-bedded shoreface deposits (coarse to very coarse sandstones) to foreshore deposits (laminated, well-sorted coarse-to-medium sandstones).

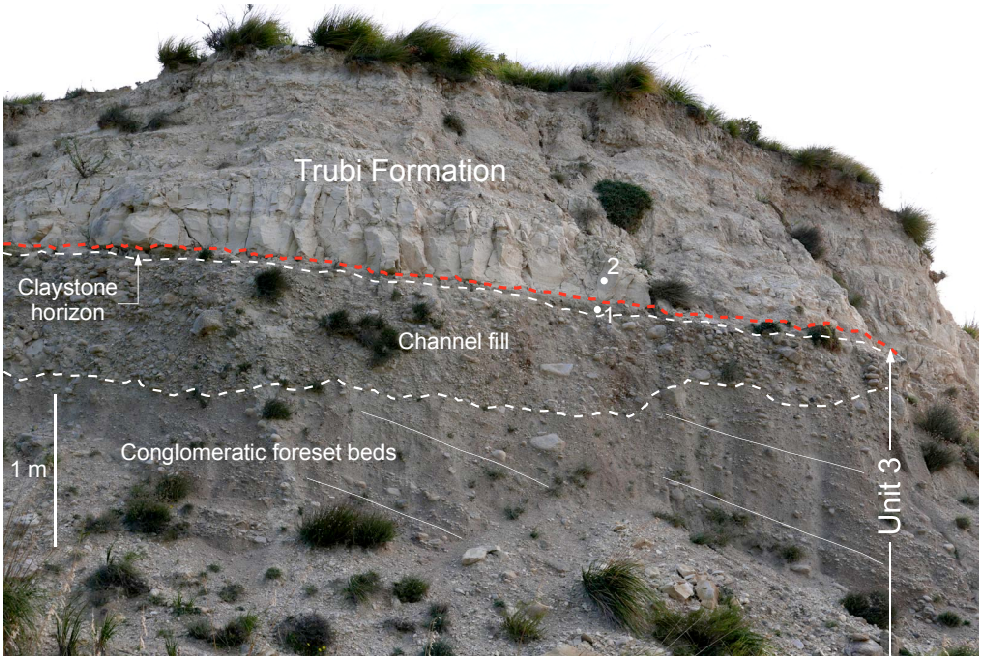

Fig. 8. Outcrop about 500 m north of the village of Careri exhibiting at its lower-half part a prograding braid-delta sequence. SE-dipping fluvial conglomerate foreset beds (delta-front deposits) of late Messinian Unit 2 are erosively overlain by channel-fill conglomerates (delta-plain deposits). The latters are in turn overlain by a thin claystone horizon closing the Unit 3 and by the cyclic whitish-grey calcilutites of the Zanclean Trubi Formation, which cover in onlap all older lithostratigraphic units in the region
White dots: studied samples.

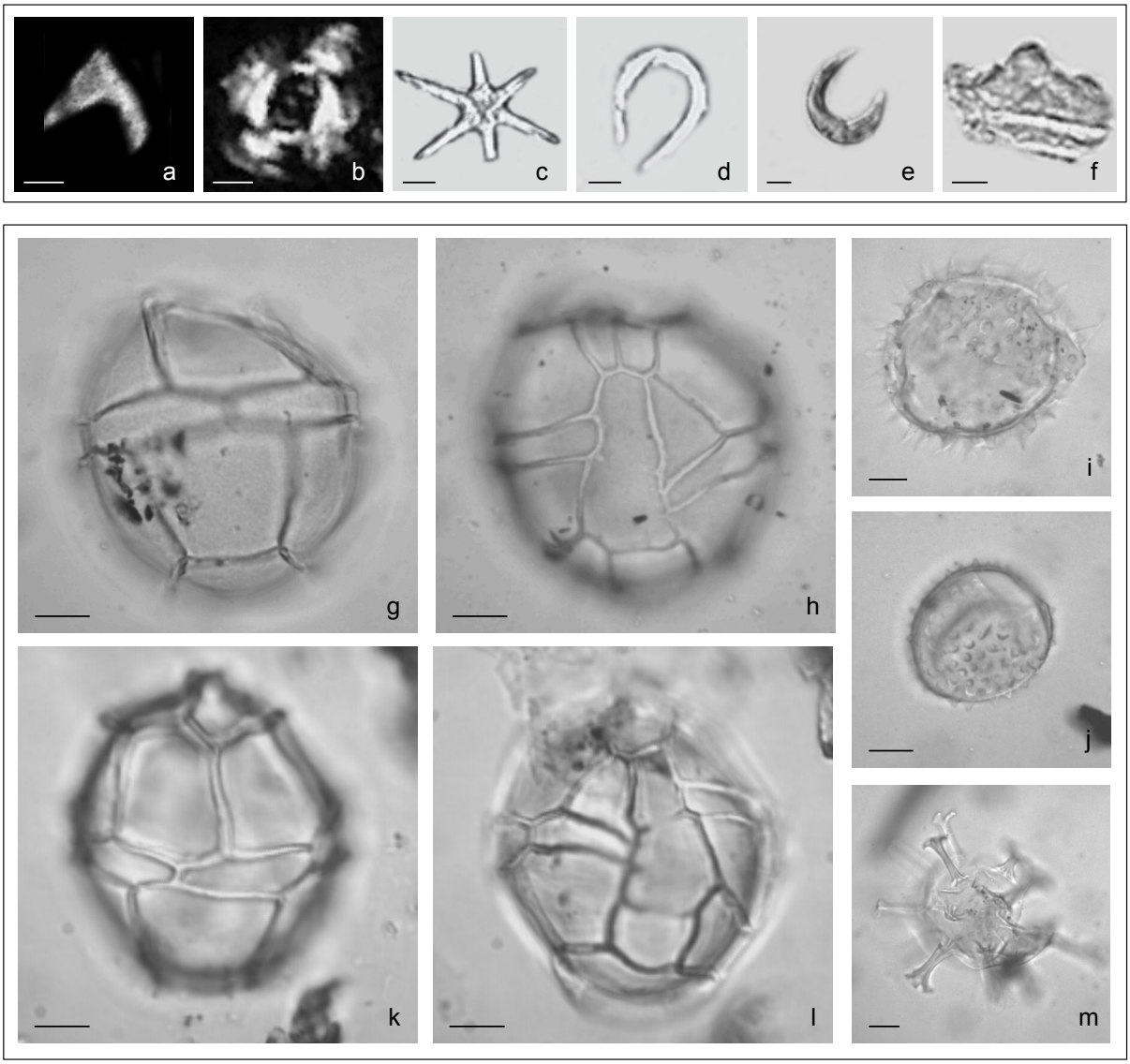

Fig. 9. Photographs of some specimens of calcareous nannofossils and dinoflagellate cysts.

a–f, Calcareous nannofossils in polarized light (scale bar = 5 μm).

a, *Ceratolithus acutus* Gartner and Bukry 1974, crossed nicols, location C4 – sample 2; b, *Reticulofenestra pseudoumbilicus* (Gartner 1967) Gartner 1969, crossed nicols, location G3 – sample 1; c, *Discoaster brouweri* (Tan Sin Hok 1927) Bramlette and Riedel 1954, parallel nicols, location C4 – sample 1; d, *Amaurolithus delicatus* Gartner and Bukry 1975, parallel nicols, location G3 – sample 1; e, *Amaurolithus primus* (Bukry and Percival 1971) Gartner and Bukry 1975, parallel nicols, location C4 – sample 2; f, *Orthorhabdus* (ex. *Triquetrorhabdulus*) *rugosus* (Bramlette and Wilcoxon 1967) Young and Brown 2014, parallel nicols, location G3 – sample 1.

g–m, Dinoflagellate cysts in natural light from location C4 – sample 6 (scale bar = 10 μm).

g–h, *Impagidinium patulum* (Wall 1967) Stover and Evitt 1978: g, dorsal view of ventral surface; h, ventral view.

i, *Lingulodinium machaerophorum* (Deflandre and Cookson 1955) Wall 1967, ventral view of ventral surface, mid focus.

j, *Operculodinium janduchenei* Head *et al*. 1989, dorsal view of dorsal surface, mid focus.

k–l, *Impagidinium sphaericum* (Wall 1967) Lentin and Williams 1981: k, dorsal view of ventral surface; l, ventral view.

m, *Homotryblium* sp. Davey and Williams 1966, right lateral view, mid focus.

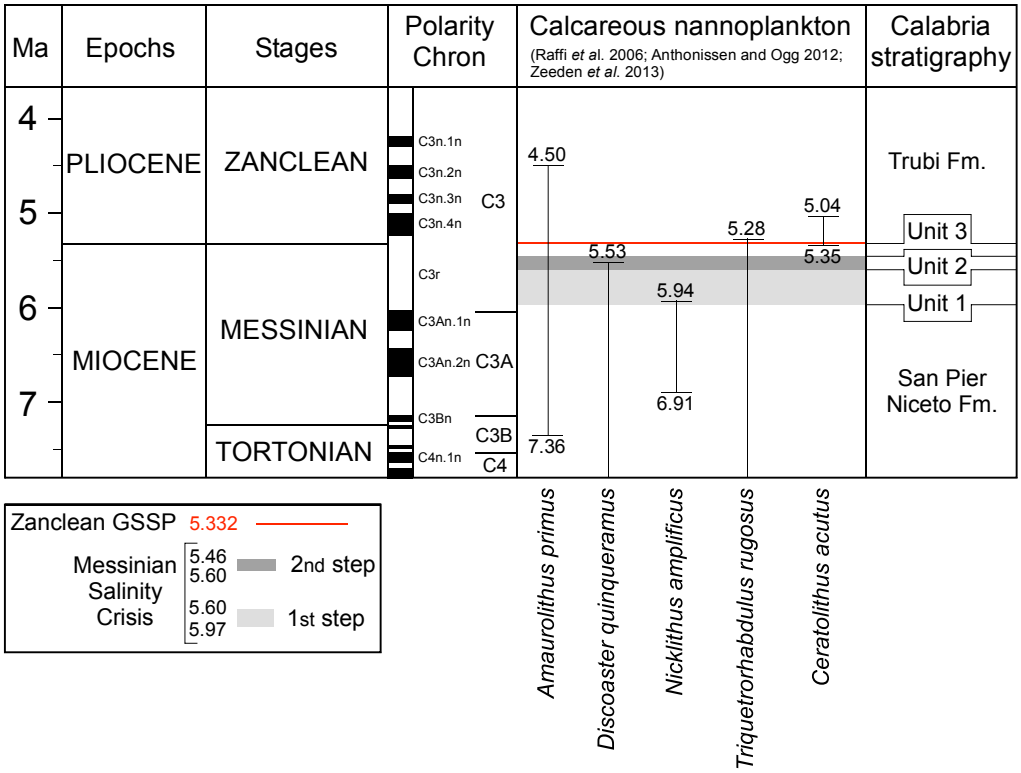

Fig. 10. Chrono-biostratigraphic chart of key calcareous nannofossil species with reference to the two steps of the Messinian Salinity Crisis (Clauzon *et al*. 1996) and the Zanclean GSSP (Van Couvering *et al*. 2000). Involvement in the Calabria stratigraphy. Polarity Chron is from Hilgen *et al*. (2012).

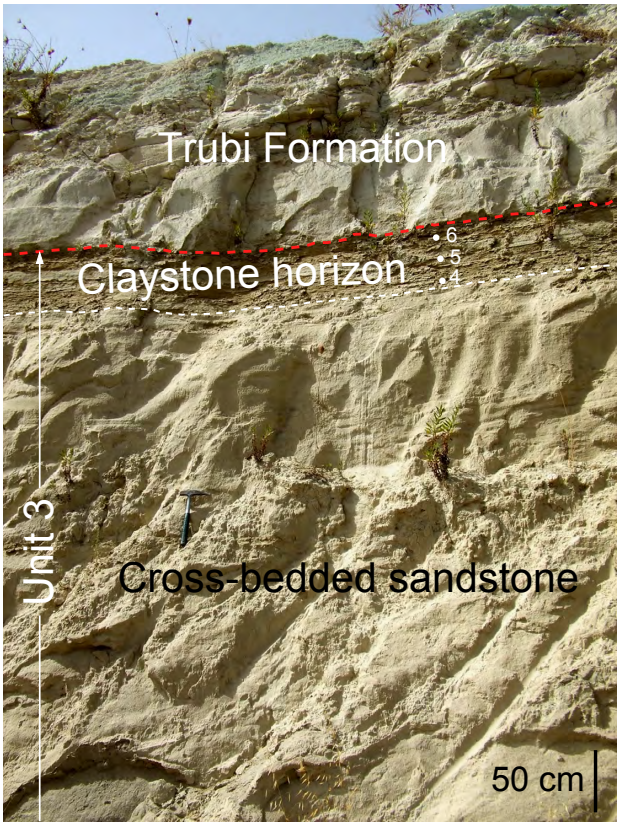

Fig. 11. View of the claystone horizon ending the Unit 3 covered by the Trubi Formation in locality C4 (see Figs. 1, 6 for location). White dots: studied samples.

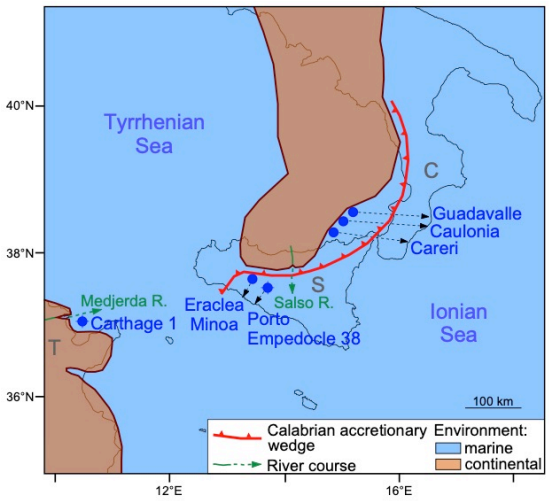

Fig. 12. Paleogeographic sketch at time of deposition of Calabrian Unit 3 and Sicilian Arenazzolo at 5.46 Ma, based on maps published by Bache et al. (2012), Henriquet *et al*. (2020), and Manzi *et al*. (2020).
Shifting of the considered locations from 5.46 Ma is arrowed by dotted black lines in the present geographic outline.
C, Calabria; S, Sicily; T, Tunisia.

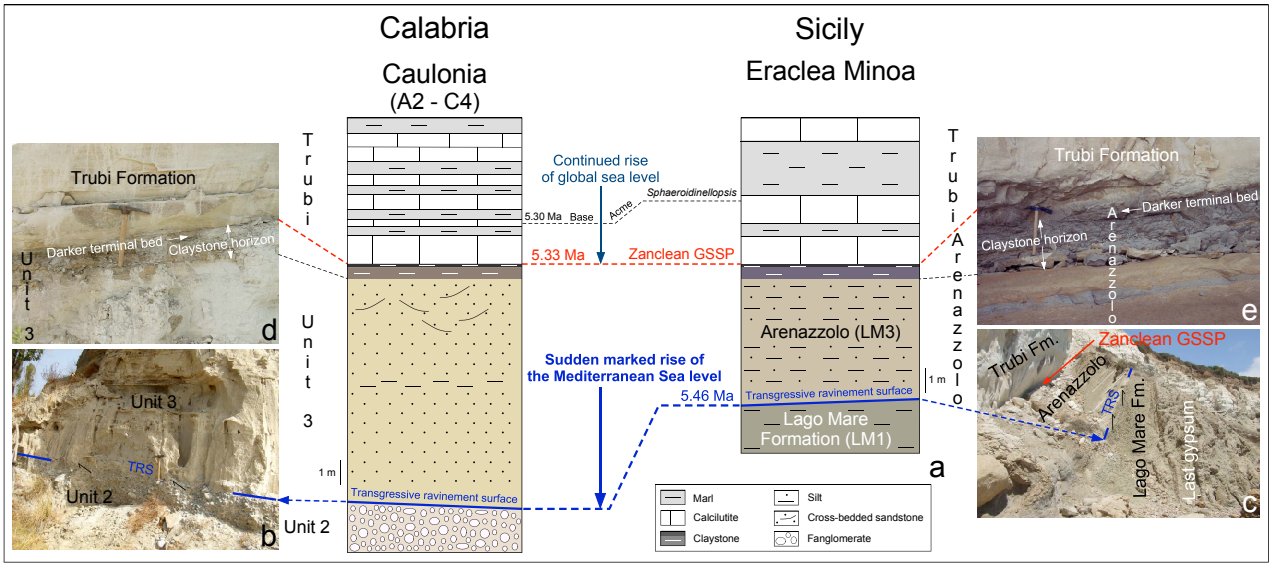

Fig. 13. Comparison of the latest Messinian–earliest Zanclean succession between Calabria and Sicily.
(**a**), Lithological successions and chronostratigraphic relationships; (**b**), Transgressive ravinement surface (TRS) marking the contact of Unit 3 over Unit 2 in the Caulonia region (location A2; Fig. 6); (**c**), Eraclea Minoa, Sicily (section of the Zanclean GSSP): TRS marking the unconformable contact of Arenazzolo over the Lago Mare Formation; (**d**), Detail of the topmost Unit 3 in the Caulonia region (location C4; Fig. 6); (**e**), Topmost Arenazzolo at Eraclea Minoa.